Title
Impoverishing Roots Will Improve Wheat Yield and Profitability Through Increased Water and Nitrogen Use Efficiencies

Journal
Journal of Geophysical Research Biogeosciences, 126(9)

ISSN
2169-8953

Authors
Woo, DK
Riley, WJ
Paez-Garcia, A
et al.

Publication Date
2021-09-01

DOI
10.1029/2020jg005829

Peer reviewed

Impoverishing roots will improve wheat yield and profitability through increased water and nitrogen use efficiencies

D. K. Woo[1], W. J. Riley[2], A. Paez-Garcia[3], A. R. Marklein[2], Z. A. Mekonnen[2], X. Liu[3], X. Ma[3], E. Blancaflor[3], Y. Wu[2]

[1]Department of Civil Engineering, Keimyung University, Deagu, 42601, Republic of Korea
[2]Lawrence Berkeley National Laboratory, Berkeley, California, 94720, USA
[3]Noble Research Institute LLC, Ardmore, Oklahoma 73410, USA

Key Points:

- Improved water and nitrogen use efficiencies were modeled when optimizing root radius and root:shoot carbon transfer conductance
- Optimizing root traits could improve wheat yields and profits without considerable nitrogen losses via nitrate leaching and N_2O emissions
- These optimized root traits imply some loss of resilience to environmental stressors, such as drought

Corresponding author: D. K. Woo, `dkwoo@kmu.ac.kr`

Abstract

More than a 60% increase in crop production is required by the 2050s to feed a growing world population. Understanding how plant functional traits and field management affect crop yields has the potential to improve agricultural productivity, minimize economic and environmental losses, and maximize food security. We explored the influence of winter wheat root characteristics and management on winter wheat growth, yield, and profit using a mechanistic and well-tested ecosystem and crop model, *ecosys*. We applied and further tested *ecosys* at an agricultural farm growing winter wheat in Ardmore, Oklahoma, United States. The model accurately predicted observed shoot carbon (R^2=0.95), soil moisture (R^2=0.67), soil temperature (R^2=0.91), and yield (percent error=17%). Numerical optimization experiments were conducted to explore potential improvements of winter wheat yield and profit by modifying root characteristics, including root radius and root:shoot carbon transfer conductance, and fertilizer inputs. Our results show the potential for simultaneously improving winter wheat yields and profits. The optimum conditions were found to be in the range of root radius between 0.1-0.3 mm, carbon transfer conductance between 0.004-0.01 h^{-1}, and the currently-applied fertilizer rate of 112 kg ha^{-1}. Under these conditions, improvements in yields and profits of up to approximately 25% and 110%, respectively, were modeled compared to those under baseline root traits. These improvements were achieved by impoverishing root structures, thereby increasing nutrient allocation to grains. Our results also demonstrate and motivate model structures that integrate the complex network of plant physiology, soil nutrient biogeochemistry, hydrology, and management.

Plain Language Summary

To meet projected food demands for a growing world population, crop yields need to be doubled by the 2050s. Although aboveground crop traits have been widely studied to improve crop yields, the "invisible" part of the crop, root systems, is not well studied. In this study, we performed a numerical optimization of root traits (such as root radius and carbon transfer conductance between shoot and root) and fertilizer application rate using a well-tested coupled ecohydrological and biogeochemical model. We found that engineering deeper wheat root structures could improve yields and profits by 25% and 110%, respectively, compared to the present day without additional fertilizer inputs. These improvements were accompanied by almost no change in nitrogen losses via surface N_2O fluxes, indicating that the optimized root traits were an environmentally friendly option to meet future food demands.

1 Introduction

Global agriculture in the 21st century will face multiple challenges to feed an expanding population (Gerland et al., 2014; Porkka et al., 2017). Meeting this demand for food while ensuring economic, environmental, and societal sustainability is a critical societal need (Godfray et al., 2010). The world population is projected to reach 9.8 billion in the 2050s, a nearly 2.4 billion rise from 2015 (Population Division of United Nations, 2017). This growth implies that agricultural productivity may need to improve by 60 to 100% to meet this increasing demand (FAO, 2009; Tilman et al., 2011). Previous studies have shown that an increase in agricultural land is possible if we convert forests and/or wasteland into productive land (Phalan et al., 2011; Fan et al., 2012; Hulme et al., 2013; Zabel et al., 2014; van Ittersum et al., 2016). However, neither of these options is optimal due to the need to conserve ecosystem services for tackling climate change and protecting biodiversity (Godfray et al., 2010; Foley et al., 2011). In view of these limitations, 21st century food security is one of the most difficult tasks that humans have faced. However, there have been tremendous improvements in crop productivity from adopting and developing more efficient and sustainable management practices, plant breeding, and transgenic crops (Miflin, 2000; Lobell et al., 2008; Bajzelj et al., 2014; Drewry et al., 2014). Such options allow society to address multiple challenges without sacrificing environmental and health assets.

During the past decades, a dramatic increase in synthetic nitrogen fertilizer production and application has contributed to improvements in crop productivity and thus alleviation of hunger (Erisman et al., 2008; Lu & Tian, 2017). Concurrently, precision agricultural practices have been devised and crops have been genetically engineered to achieve greater yields through an improvement in water and nitrogen use efficiency (Koziel et al., 1993; Karp et al., 1997; Linquist et al., 2013; Geng et al., 2015; Lopes et al., 2018; Woo & Kumar, 2017, 2019). In general, wheat genotypes with deeper roots require a relatively smaller amount of nitrogen fertilizer for their growth due to physiological advantages in uptaking water and nitrogen (Oyangi, 1994; Foulkes et al., 2011; Cormier et al., 2016). In addition, there has been a gradual decrease in root biomass of wheat varieties introduced over the last 50 years to increase yields by reducing nutrient allocations to root growth (Aziz et al., 2017).

Crop yield maximization has been widely used and supported (Vandermeer, 1998; Prasad et al., 2002; Islam. & Talukdar, 2014; Tripathi et al., 2016; Wang et al., 2017). In practice, however, the demand for greater yield is complicated by concurrent economic challenges (Pannell, 1999; Vico & Porporato, 2011; Doi & Pitiwut, 2014). That is, maximization of wheat yields does not necessarily guarantee economic benefits to farmers, thereby not encouraging them to adopt the optimized cultivar and management practices in a timely manner. This conflict is in part due to the high cost of nitrogen fertilizers (Edgerton, 2009; Vercruyssen et al., 2015) and weather fluctuations (Lobell et al., 2011; Frieler et al., 2017), which elevate uncertainty of operational costs and revenue associated with crop productivity (Pannell, 1999; Kihara et al., 2016). Therefore, a holistic approach to the improvement of both wheat yields and profitability is necessary to improve efficiency of innovation adaptation and reduce negative environmental consequences. There are a few studies that proposed wheat yield optimizations from an economic perspective (e.g., Zhang et al. (1999); Gandorfer and Rajsic (2008); and Malve et al. (2016)). However, a complete evaluation of fertilizer amounts and costs, simultaneous optimization of root structural and functional characteristics for improving wheat yields and profitability, and their environmental sensitivity and consequences, is lacking. Performing such an evaluation is the goal of this study.

Wheat is one of the most widely grown cereal crops (along with rice and maize) in terms of global production, providing approximately 20% of calories and protein required by the world population (Gill et al., 2004). In particular, it is the most important food crop cultivated in and exported to developing countries as the first sources of protein (Braun et al., 2000). By 2050, wheat production will need to increase by at least 60% to mitigate risks of food shortages in low-income countries (Rosegrant & Agcaoili, 2010). The process by which wheat productivity is optimized therefore affects the quality and protection of human health. In this context, exploring the potential of improving wheat productivity and profitability will play a critical role in supporting the growing demand for plant-based food.

As noted by Herder et al. (2010), most previous genetic studies have focused on the impacts of aboveground plant traits, such as leaf angle (Araus et al., 1993; Lonbani & Arzani, 2011), leaf albedo (Drewry et al., 2014), and specific leaf area (Richards., 2000; Rebetzke et al., 2004; Sieling et al., 2016), on wheat productivity. The "invisible" part of the crop, root systems, has not been not well studied in recent research. In this context, we have examined whether winter wheat could be restructured to improve grain production under different crop management practices while increasing overall profit. In particular, we address the following questions: (1) which, and to what extent, can root traits be engineered to optimize yields?, (2) how much fertilizer does the engineered cultivar require?, and (3) how do trait optimizations for yield and farmer profit differ? To explore these questions, we further tested and then conducted numerical optimization experiments with a well-tested coupled ecohydrological and biogeochemical crop model, ecosys. We varied (1) two root characteristics (root radius and carbon transfer conductance between root and shoot) and (2) fertilizer application rates. By taking advantage of this well-established and widely-validated model that has been tested across space and time (Grant., 1991; Grant et al., 1995, 1999, 2011; Webber et al., 2017; Mekonnen et al., 2018; Woo et al., 2020), we attempt to uncover novel insights into the potential of engineering wheat root traits for improving productivity and profitability and thus inform breeding programs.

2 Materials and Methods

2.1 Model testing sites

To assess the robustness of model predictions, we compared model results with observations available at site and regional scales. This validation procedure aims to build confidence in conclusions drawn by numerical optimization experiments conducted in this study.

2.1.1 Site level observations

The main study site is an active experimental farm in Ardmore, Oklahoma, United States (34° 11′ 8.88″ N, 97° 5′ 12.48″ W). The soil type is clay loam with a pH of 5.9. Soil cores with a 0.05 m diameter and 1 m length were sampled to measure bulk density. Long-term average annual precipitation and temperature are 960 mm and 17 °C, respectively. This site experiences considerable seasonal variations in both precipitation and temperature driven by the polar and subtropical jet streams. The precipitation distribution throughout a year typically has peaks in late spring and early fall (Eddy, 1982). The average daily temperature ranges between 0 °C in winter and 28 °C in summer. Over the past 25 years (1994–2018), hourly weather forcing data to run the model (i.e., precipitation, air temperature, incoming solar radiation, humidity, and wind speed) were collected from a local weather station from Weather Underground and the National Solar Radiation Database.

We conducted two growing seasons field experiments from 2016 to 2018; (i) 2016-2017 (hereafter referred to as the 2016 season); and (ii) 2017-2018 (hereafter referred to as the 2017 season). In the 2016 season, winter wheat (Duster) was planted on October 30 and in the 2017 season it was planted on October 10. A disked-tillage treatment was applied to a depth of 0.1 m for plow tillage in September during both seasons. To meet nitrogen requirements for winter wheat production, 56 kg N ha^{-1} nitrogen fertilizer was applied twice in October as pre-plant urea ammonium sulfate and in January as a broadcast application. Aboveground and belowground biomass was sampled five times during the two growing seasons and used to estimate winter wheat carbon contents per unit area for model testing. Shoot biomass was measured on 1/30/2017, 1/1/2018, and 3/7/2018, and top 0.25-m root biomass was measured on 1/30/2017 and 4/11/2018. The shoot biomass was measured after leaf emergence and 8-weeks after that. To monitor the temporal variations of soil moisture and temperature, ten Decagon 5TE sensors were sparsely installed at 0.3 m depth in October 2017. No irrigation, insecticide, or fungicide were applied during the two seasons.

To augment these benchmark observations for further model evaluation, we obtained observed aboveground carbon stocks of winter wheat grown in Ponca City, Oklahoma from 1998 to 2000 from published experimental data (Kocyigit & Rice, 2004). Our model validation using the same wheat cultivar (Duster) from an adjacent region and period demonstrates that the model simulations of phenomenological behavior and biomass dynamics are robust for soils, climate, and crop types in the region.

2.1.2 Regional scale observations

The purpose of validation exercises at the regional scale is to establish whether processes governing modeled crop yields associated with parameters used in this study allow for a reasonable agreement with spatially distributed yields. In Oklahoma, there are five agricultural districts (Northwest, Southwest, Central, Northeast, and Southeast) classified based on similar agricultural characteristics, such as soil fertility, fertilizer application rates, and flowering time, to allow comparisons of heterogeneous agricultural productivity. Our main study site, Ardmore, belongs to the Central agricultural district. Therefore, winter wheat grain yields available from the agricultural region for the last 20 years (1998 to 2017) from the National Agricultural Statistics Service (NASS) were obtained and compared with model predictions. Here, to convert unit of measure from bushels acre^{-1} to g m^{-2}, we used a unit convertion factor of 6.725 for wheat based on Weiland and Smith (2013).

2.2 *Ecosys* model description

2.2.1 General overview

Ecosys is a sub-hourly time-step ecosystem model, coupling ecohydrological and biogeochemical dynamics by solving coupled relationships between energy, water, carbon, nitrogen, and phosphorus dynamics of multi-layer plant canopies and soils. This model is designed to represent terrestrial ecosystems ranging from natural to managed systems and has been widely applied across different climate regions and vegetation types in over 90 publications(e.g., Grant. (1991), Grant et al. (1995, 1999, 2011), and Webber et al. (2017)). This model has been applied to and validated for wheat growth and associated nitrogen dynamics, including N2O emissions, in several agricultural systems (Grant., 1991; Grant et al., 1995, 1999, 2011; Webber et al., 2017). Below, we briefly describe relevant key equations and algorithms associated with root, nutrient, and water dynamics. A detailed description of inputs, parameters, and algorithms used in ecosys is provided in Grant (2013). A schematic diagram of the model is presented in Figure A1 in the Appendix. The model, parameters, drivers, and outputs used in this study are placed in an online repository (`https://github.com/dwoo5/ECOSYS`). Readers that wish more detailed descriptions of the processes are referred to the Supplemental Material in Grant (2013).

2.2.2 Root growth

Root growth: The root system in *ecosys* is represented with two main root types: vertical primary and horizontal secondary roots growing from different stem nodes of each plant functional type (Grant, 1998). The distribution and amount of roots control the dynamics of plant O_2, water, and nutrient uptake (Grant., 1991; Grant, 1993b, 1993a), and thus influence plant growth processes, such as photosynthesis, respiration, and transpiration. Here, we briefly describe the overall algorithmic structure of the primary root growth implemented in the model. The biomass of the primary root (M_r, g m^{-2}) is estimated by combining its growth respiration (R_G, g m^{-2} h^{-1}), specific growth respiration (R_g, g g^{-1}), and senescence (R_d, g m^{-2} h^{-1}):

$$\frac{\partial M_r}{\partial t} = R_G \frac{1 - R_g}{R_g} - R_d \tag{1}$$

where

$$R_G = \begin{cases} R_T f_\psi, & \text{if } R_T f_\psi \leq \frac{J_s}{\sum J_s} R_g f_{np}. \\ \frac{J_s}{\sum J_s} R_g f_{np}, & \text{otherwise.} \end{cases} \tag{2}$$

R_T is total root respiration under no water limitation (g m^{-2} h^{-1}); f_ψ is a water constraint affected by root water potential, turgor pressure, and soil resistance (MPa); J_s

is root conductance to carbon, nitrogen, or phosphorus; f_{np} represents a nitrogen or phosphorus constraint for the root growth respiration:

$$f_{np} = \begin{cases} \frac{Z_n}{C_n(1-R_g)}, & \text{if } \frac{Z_n}{C_n(1-R_g)} \leq \frac{Z_p}{C_p(1-R_g)}. \\ \frac{Z_p}{C_p(1-R_g)}, & \text{otherwise.} \end{cases} \tag{3}$$

where Z_n and Z_p are nitrogen and phosphorus storages in root, respectively (g m^{-2}); and C_n, and C_p are nitrogen and phosphorus concentrations maintained by root biomass, respectively (g g^{-1}). I.e., the respiration rate of primary root growth is constrained by water, carbon, nitrogen, and phosphorus content.

Root:Shoot nutrient transport: The flux of nutrient movement between roots and shoots (F_{sr}, g m^{-2} h^{-1}) for their growths is driven by the concentration gradient (Brugge & Thornley, 1985):

$$F_{sr} = g_c \frac{\sigma_b M_r - \sigma_r M_b}{M_r + M_b} \tag{4}$$

where g_c is a nutrient transfer conductance between root and shoot (h^{-1}); σ_b and σ_r are non-structural carbon from CO_2 fixation or non-structural nitrogen or phosphorus from root uptake in branches and roots, respectively (g g^{-1}); and M_b is the branch biomass (g m^{-2}). In general, the direction of carbon transfer occurs from shoots to roots while nitrogen and phosphorus transfers occur in the opposite direction. The amount of nitrogen and phosphorus in leaves affects the CO_2 fixation rate from sunlit and sun-shade leaf surfaces (Grant, 2013). On the other hand, the amount of carbon in roots influences the rate and pattern of water and nutrient uptake from the soil (Grant, 1998).

2.2.3 Soil water and nutrient transport

Surface water: Precipitation (P, m^3 m^{-2} h^{-1}) is separated into four components: surface water ponding (d_w, m^3 m^{-2}), surface water runoff (Q_r, m^3 m^{-2} h^{-1}), evaporation (E, m^3 m^{-2} h^{-1}), and infiltration (Q_w, m^3 m^{-2} h^{-1}):

$$\frac{\partial d_w}{\partial t} = Q_r + P - E - Q_w \tag{5}$$

where

$$Q_r = \left(R^{0.67} \frac{s_r^{0.5}}{z_r} \right) d_m L \tag{6}$$

where the equation in parentheses represents runoff velocity (m h^{-1}), which is estimated using the ratio of cross-sectional area to perimeter of surface flow (R, m), slope of channel side during surface flow (s_r, m m^{-1}), and Manning's roughness coefficient (z_r, m$^{-1/3}$ h). The surface water runoff is calculated as the product of runoff velocity, and depth (d_m, m) and width (L, m) of mobile surface water.

Subsurface water: The variables predicted from the subsurface water dynamics, such as subsurface water fluxes and soil moisture, are used to drive plant phenological and biogeochemical dynamics directly through the effect of water on carbon uptake and decomposition and indirectly through the effect of water on nitrogen uptake and soil temperature. The subsurface moisture flow is modeled using Richards' equation (Richards, 1931).

Solute transport: The transport of solutes, such as ammonium, nitrate, and dihydrogen phosphate, in soil media, is modeled using the advection-dispersion equation (Grant, 2013). The diffusivity is estimated as a function of water-filled porosity, tortuosity, and soil temperature.

2.3 Simulation protocol

To minimize the influence of initial soil water, temperature, nutrient, and vegetation conditions on model predictions, we performed a 50 year spin-up prior to 1998 with the same wheat crop and fertilizer management as during the experiment. Since observed weather data is unavailable for the spinup period before 1993, we used a stochastic weather generator (Fatichi et al., 2010) with parameters estimated based on the observed 25 years of weather data, including precipitation, temperature, humidity, wind speed, and solar radiation (Figure A2). The stochastic weather generator produced hourly metrological variables that were statistically equivalent to observed weather input data. Soil and wheat parameters used in this study were obtained from previous experimental and numerical studies (Table 1). Other parameters not listed in Table 1 were obtained from previous wheat studies and default values (Grant, 1998, 2013; Grant et al., 2011). The upper boundary condition at the top of the canopy is formulated by weather forcings while the lower boundary condition at the bottom of the soil is set as a partially permeable layer assuming 10% free drainage flux. Capillary rise from the layer beyond the bottom is ignored.

3 Results

3.1 Model performance

We first compared the model responses with observed data available for shoot carbon, root carbon, soil moisture, and soil temperature at site levels. The model accurately predicted observed soil moisture and temperature, and shoot and root carbon over the model validation period from 1998 to 2018 (Figure 1a,b). The predicted aboveground carbon closely matched observed trends in 1998, 1999, 2000, 2017, and 2018 (R^2=0.95; Figure 1c). Although root carbon stocks were measured only one time per year, the predicted biomasses matched very closely with the observations (Figure 1d).

At the regional scale, we conducted a comparison between mean observed NASS Central agricultural district and modeled Ardmore grain yields from 1998 to 2017 (R^2=0.36; Percent Error=17%; Figure 1e). A possible explanation for the gap between predicted yields and the NASS survey-reported yields is that the NASS survey data are spatially-averaged yield data over variations in multiple winter wheat cultivars (more than 40 cultivars), soil types, topography, and fertilization application rates. Despite these differences between observed and modeled conditions, more than 75% of the predictions fell within the range of the observed data. In general, the modeled results agree well with the observed data at site and regional scales, providing confidence to use the model to evaluate the influences of root characteristics on winter wheat growth and yield.

3.2 Root traits optimization

We applied the tested model to examine whether winter wheat could be engineered to improve the amount of grain produced per unit area under present-day crop management practices and climate conditions. To explore this question, we conducted numerical optimization experiments by varying two root characteristics: root radius and carbon transfer conductance between root and shoot. These parameters were chosen since they are identified as sensitive and important parameters to characterize root systems based on a sensitivity analysis conducted for this model (Grant, 1998). The root radius and carbon transfer conductance were free parameters in the optimization experiments and were allowed to vary within the range 0.05-1 mm and 0.002-0.04 h^{-1}, respectively. These ranges were determined based on previous experimental studies (Grant, 1998; Munoz-Romero et al., 2010; Ward et al., 2011; Fricke et al., 2014; Colombi et al., 2017; Dal Cortivo et al., 2017; Liu et al., 2018). To have statistically meaningful and reliable results, we conducted the model simulations for 50 years after model validation by varying (1) root radius only, (2) root:shoot carbon transfer conductance only, and (3) all togethor. Weather forcings associated with these numerical experiments were generated based on the 25 years of observed weather data as described in the Methods.

Independently increasing root radius or decreasing carbon transfer conductance from the baseline values increased modeled winter wheat yields (Figure 2a, b). However, in this single-objective optimization sensitivty analysis, a wide optimization range for the root radius is observed (0.5-0.8 mm), indicating that the root radius may not be an important root trait. That is, parsimonious root structures increased wheat yields by improving nutrient allocations to grains during grain filling. Overall, the increased yields occurred with relatively parsimonious root structures that allow the crop to allocate more nutrients to grain during grain filling by limiting nutrient allocation to roots. However, excessively poor root structures also lead to water and nutrient-limiting conditions, inhibiting crop growth and metabolism in some years. We note that a sharp reduction in yield is modeled when each root trait independantly is small (smaller than 0.1 mm root radius and 0.004 h^{-1} carbon transfer conductance). That is, the crop with the single-parameter optimized root structures improved grain yields while losing some resilience to environmental stress, such as drought and nutrient deficiency, and increasing the possibility of crossing a threshold from a desirable to an undesirable stable state.

When the two root chracteristics were simultaneously optimized for optimal winter wheat yields (Figure 2c), the maximum yields (95^{th} percentile) occur in the range of root radius between approximately 0.1-0.3 mm and carbon transfer conductance between 0.004-0.01 h^{-1}. Within the optimized yield cases (red area in Figure 2c, d), the root distribution depth was deeper and root biomass was lower compared to the case under baseline root traits (Figure 2e). We also note that a linear superposition of yields arising from the single root trait changes does not lead to the multi-parameter optimal solution. That is, objective functions are partially interdependent and thus they converge to minimal root structures necessary in response to water and nitrogen stress. This argument is also supported by an increase in modeled water and nitrogen use efficiency (defined as grain carbon yield per unit water and nitrogen uptake, respectively) under the case for the optimized root traits compared to that for baseline root traits (Figure 3). Using a standard conversion factor to estimate grain protein (Merrill & Watt, 1973; Spitzer et al., 1996), a slight but not significant increase in protein with the optimized root traits ($<1\%$) is also modeled due to a corresponding increase in grain nitrogen.

Inter-annual variability for the optimized yield cases is relatively higher than that for baseline root traits (Figure 4a). To explore the associated dynamics in yield inter-annual variability, we examined the relationship between precipitation and winter wheat yields. We applied the 3-month Standardized Precipitation Index (SPI) (Hao & AghaKouchak, 2014) (Figure A3), which is a widely used proxy to characterize the extent of dry and wet conditions in agricultural systems (Guttman, 1998). The magnitude of negative and positive SPIs represents the intensity of drought and wetness, respectively. We found, after dry winter periods (the three months ending in January (SPI-Jan) and February (SPI-Feb), winter wheat yields under optimized root traits were higher than under the baseline scenario (Figure 4b, c, A4). Simulations indicate that, in low precipitation winters, soil nutrient losses are reduced (via leaching and N_2O emissions), allowing the optimized crop to uptake more nutrients due to the greater rooting depth.

3.3 Economic analysis with fertilizer application

We next explored the effects on winter wheat yields with combinations of primary root radii and root:shoot carbon transfer conductances and fertilizer application rates of 0, 56, 112, 168, and 224 kg ha^{-1} yr^{-1} as pre- and post-plant fertilization on the same date as for the previous model experiments. The range of fertilizer application rates was decided based on present-day winter wheat fertilizer application rates in the United States

(Mueller et al., 2013), and we chose 0, 25, 50, 75, and 100% of that range for this sensitivity analysis.

As expected, the results show that winter wheat yield increases as the fertilizer application rate increases within the experimental range (Figure 5a, c). The maximum yields occur under the optimized root traits at each fertilizer application rate (red area in Figure 5a, b). In particular, the consistency and robustness of the optimized root traits are observed and maintained regardless of fertilizer rates.

Following Vico and Porporato (2011), an economic analysis was performed to analyze tradeoffs between yield and economic return. Gross income per unit area can be determined by wheat yield (Y) multiplied by wheat sale price (c_s) plus grazing return (G_g). The cost of wheat cultivation can be classified into two main components in rainfed agricultural systems: (i) fixed cost per unit area (C_0) for land, seed, insurance, labor, and field machinery, and (ii) fertilizer cost that is determined by the amount of fertilizer applied (F) multiplied by fertilizer sale price (c_f). That is, profit per unit area (G_n) can be expressed as:

$$G_n = c_s Y + G_g - C_0 - c_f F \tag{7}$$

Here, for the sake of simplicity, we assume that the fixed cost is not influenced by fertilizer amount applied and grazing return is constant. We recognize that more complex economic analyses can be performed, but considering these factors provides a good estimate of tradeoffs associated with fertilizer application rates and costs. For the parameterization of the above economic balance for the case of winter wheat, we followed the economic analysis of wheat production in Oklahoma (DeVuyst, 2012) for the fixed cost (145.2 \$ acre^{-1}) and grazing return (90.45 \$ acre^{-1}). However, we note the wide fluctuations of wheat and fertilize sale prices over the last decade. Based on data from the U.S. census (USDA, 2019a, 2019b; Macrotrends, 2019), U.S. wheat sale prices ranged from 3.90 to 9.40 \$ bushel^{-1} and urea fertilizer prices ranged from 0.35 to 0.85 \$ acre^{-1}. Thus, we assumed averaged wheat sale price, 5.8 \$ bushel^{-1}, and fertilizer price, 0.45 \$ acre^{-1}, and conducted a sensitivity analysis over the ranges of wheat and fertilizer sale prices as described in Section 3.5.

We found that economic profitability does not scale linearly with increased wheat productivity resulting from increased fertilizer application rate (Figure 5b, d). Under baseline root structures, the maximum profit occurs at the same amount of fertilizer currently applied at the study site (112 kg ha^{-1} yr^{-1}), to a certain degree consistent with the stagnation of winter wheat yields since the 1990s (Wiesmeier et al., 2015). Under the optimized root structures, the maximum profit does not occur where winter wheat yield is at a maximum because producing at the point of maximum yield requires relatively high quantities of nitrogen fertilizer. Rather, the optimum amount for nitrogen fertilizer from an economic perspective is estimated to also be at the rate currently applied at the study site. Compared to the case for baseline root structures, profit improves by approximately two times under optimized root structures (Figure 5d). We also note that profit under optimized root structures does not increase with additional fertilizer past the optimal 112 kg ha^{-1} yr^{-1} rate.

3.4 Environmental effects

To explore the environmental effects of the optimized root traits and fertilizer management, we quantified gross primary productivity (GPP), autotrophic respiration (R_a), net primary productivity (NPP), leaf area index, soil organic carbon, and soil organic nitrogen, nitrogen leaching at a depth of 2 m, and soil nitrous oxide (N_2O) fluxes for the maximum yield and profit scenarios (Figure 5e, f, g, and Figure A5). We modeled a decrease in GPP, R_a, NPP, leaf area index, soil organic carbon, and soil organic nitrogen under both scenarios compared to the baseline scenario. These decreases are mainly due to reduced GPP caused by limiting nonstructural nitrogen and phosphorus transfer from root to shoot under the optimized root structures, leading to decreases in photosynthesis. However, the optimized root structures allocate more nutrients to wheat grains by not utilizing the resources for root growth. These dynamics are also explained by the increased fraction of GPP that supports R_a under optimized root structures (Figure A5c). In addition, the increased nitrogen fertilizer application rate for the maximum yield case and the improved nitrogen use efficiency for both cases lead to a slight increase in nitrogen leaching from the system (Figure 5f). Similarly, a slight increase and decrease in soil N_2O fluxes for the maximum yield and profit cases, respectively, were modeled (Figure 5g). These N_2O fluxes are about equivalent to releasing and reducing 57 g and 43 g of CO_2, respectively. These results indicate that there is a need to account for the environmental costs along with the potential for increasing food production to meet future demand.

3.5 Sensitivity analysis of wheat profit

We next analyzed the impacts of inter-annual variability in wheat and fertilizer sale prices on wheat profitability (Figure 6a, b). Results for a root radius of 0.1 mm and carbon transfer conductance of 0.006 h^{-1} were presented since the maximum profit occurs with the optimized root structures (Figure 5b). The different combinations of wheat and fertilizer sale prices result in different nitrogen fertilizer requirements to maximize profit. When fertilizer sale prices are higher than present day, a reduction in fertilizer applications becomes more profitable, but with a gradual decrease in revenue. The opposite is true for the case of wheat sale prices higher than present day. In particular, the maximum profit increases with increasing wheat sale price accompanied by increased application rates of fertilizer. This relationship occurs because the increase in fertilizer use is offset by increasing gross income due to the high value of winter wheat. However, fertilizer use efficiency, which is defined as yield per unit fertilizer input, becomes lower as fertilizer use becomes higher (Figure 6c). At low wheat and high fertilizer sale prices, the maximum profit is achieved when no fertilizer is used. We note that under the assumptions of the fixed cost and grazing return, the normal profit (defined as a condition when a farmer's gross income is equal to total cost) occurs at a wheat sale price of 3.1 \$ $bushel^{-1}$ indicating that a lower wheat sale price may result in a scenario where abandoning the harvest produces the optimal profit outcome.

4 Discussion

Optimum crop yield depends on maintaining effective coordination between shoots and roots for plant growth. That is, the growth of shoots should not be sacrificed to deficiencies in essential nutrients supplied by root reserves, and vice versa (e.g., Long et al. (1994, 2006); Sinclair and Rufty (2012); and Ortez et al. (2018)). In this view, reduced root growth can lead to an increase in yield, when crops are not subjected to stress such as insufficient soil water and nutrients, due to a functional equilibrium between above- and below-ground utilization of resources (Brouwer, 1962; D. Richards, 1978; Feller et al., 2015). Several previous studies, including in other cereal crops such as maize and rice, have found a concave relationship between grain yield and root dry weight (Fageria et al., 2011; Aziz et al., 2017; Islam et al., 2019). In addition, it has been widely reported that a deeper root system is beneficial for maintaining and improving crop productivity through efficient water and nitrogen acquisitions, thereby reducing drought stress and nitrogen deficiency (Dunbabin et al., 2003; Ao et al., 2010; Ju et al., 2015; Li et al., 2016). Consistent with these findings, our results also show that these properties can be achieved by genetically engineering winter wheat root radius and root:shoot carbon transfer conductance. We found that the optimum conditions were in the range of root radius between 0.1-0.3 mm, carbon transfer conductance between 0.04-0.01 h^{-1}, and current fertilizer input rate (112 kg N ha^{-1}). Under these conditions, improvements in yield and profit of 25% and 110%, respectively, were attained compared to those under baseline root traits (Figure 3 and 5). These findings indicate the potential for crop breeding methods to increase yields.

Plants do not operate at maximum capability because, e.g., they save resources to cope with unexpected environmental stress (Natarajan & Willey, 1996; Lin, 2011; Srinivasan et al., 2016). For example, Srinivasan et al. (2016) found that a decrease in peak leaf area index of 38% led to an increase in yield of 8% due to a reduction in leaf tissue construction and maintenance costs. Analogously to that study, our results show that improvements in yield were achieved by limiting nutrient allocation to root systems, thereby increasing resource allocation to grains during grain filling. However, we also noted a sharp reduction in yield (from the optimum) with slightly reduced root radius and carbon transfer conductance outside of the optimum range, resulting from adverse environmental factors such as drought and nutrient deficiency in some years. That is, improved profitability was achieved at the expense of losing some resilience of crop productivity. However, precision agricultural practices coupled with improvements in crop breeding and genomics for pest and pathogen resistances have been alleviating such side effects (e.g., Woo and Kumar (2017) and Lynch (2018)).

An increase in nitrogen fertilizer application often results in crop yield increases by mitigating nitrogen-limited environments in the root zone (Erisman et al., 2008; Lu & Tian, 2017; Ortez et al., 2018). However, the excessive use of fertilizer leads to elevated nitrogen losses to receiving water bodies (Li et al., 2010; Radcliffe et al., 2015; Woo & Kumar, 2016; Sinha et al., 2017) and the atmosphere as volatilization (Good & Beatty, 2011), causing consequent environmental degradation and economic losses to farmers (Goulding et al., 2008). These negative consequences occur because only one-third of nitrogen fertilizer applied to the soil is taken up by crops (Raun & Johnson, 1999; Gardner & Drinkwater, 2009; Ciampitti & Vyn, 2014) and fertilizer use efficiency decreases as the use of fertilizer increases (Ray et al., 2013). Therefore, the use of nitrogen fertilizer also needs to be considered while meeting the growing demands of plant-based food. In this study, we show that there is potential to simultaneously improve crop grain yields and profits without a significant increase in nitrogen leaching by “impoverishing, not enriching”, root systems (Figure 5). That is, solely increasing fertilizer applications for yield improvement is not a sustainable option to increase crop yields.

This study considered only a single crop, winter wheat, to explore whether root structures can be redesigned to meet growing global food demands by improving yields and profitability per unit land area. To extend our results in future analyses, we recommend that impoverished root structures be examined further to assess the impacts of climate change, soil properties, and field management on wheat yields. However, our results indicate that developing relatively more impoverished root systems will enhance nonstructural nutrient allocations to grains. A recent review paper (Lynch, 2018) also argued that parsimonious root structures were advantageous to improve crop yields in high-input agricultural systems. Genetically engineering root radius and carbohydrates transfer conductance between shoots and roots should be tested. Therefore, in light of the findings obtained in this study, we conclude that the concept of “impoverishing, not enriching” root systems may improve winter wheat profitability albeit with the potential for rainfed crops to be more susceptible to drought.

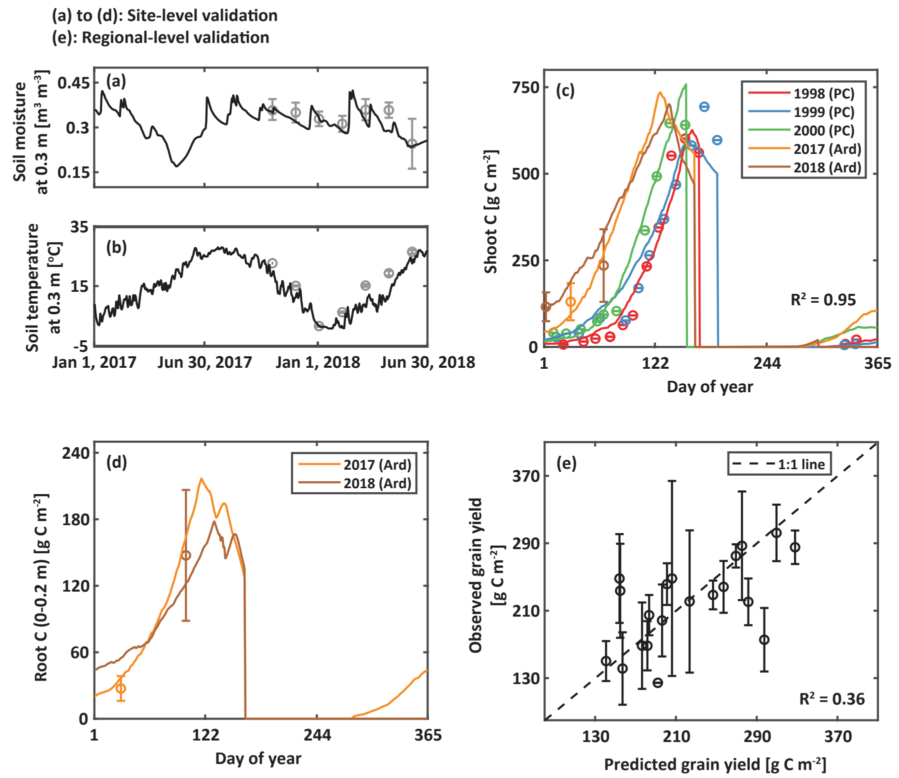

Figure 1: For site-level validation, (a) predicted (solid lines) and observed (circles and circles with error bars) soil moisture, (b) soil temperature, (c) shoot carbon (R^2=0.95), and (d) root carbon to a depth of 0.2 m during the model validation period. For regional-level validation, (e) 1:1 plot for the observed and predicted grain yields from 1998 to 2017 (R^2=0.36). PC and Ard in (c) and (d) represent data from Ponca City and Ardmore (study site), respectively. Error bars represent standard deviations. Note that observed shoot carbon in 1998, 1999, and 2000, which were taken from an adjacent site (Kocyigit & Rice, 2004), did not report error bars. The different colors in (c) and (d) represent different growing seasons.

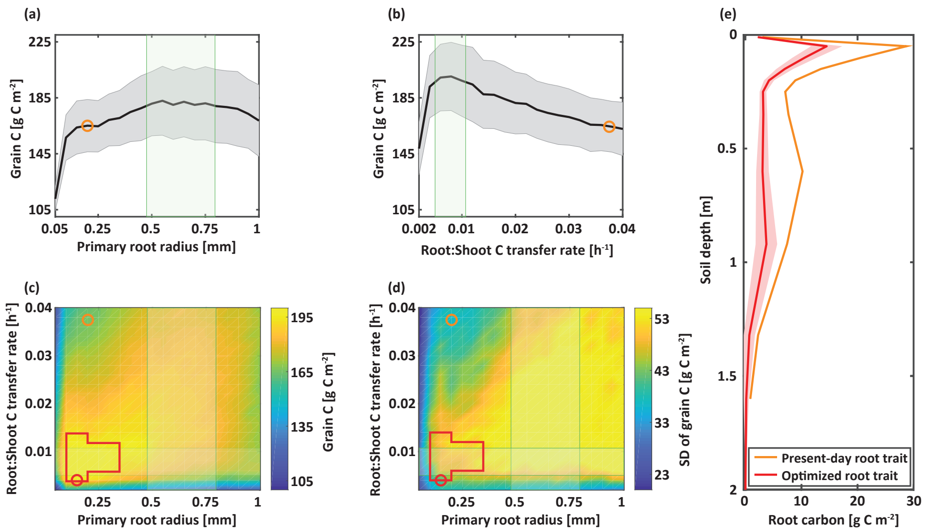

Figure 2: Modeled winter wheat yield by varying (a) primary root radius alone, (b) root:shoot carbon transfer conductance alone, and (c) both parameters together. (d) is the standard deviation for the simulations under (c). The total simulation period is 50 years. The black solid line and shaded gray area in (a) and (b) represent the average and standard deviation of winter wheat yields, respectively, across the tested parameter range. The orange circles and red circles are parameters from baseline and optimized simulations, respectively. Green shaded regions in (a) and (b) represent areas within plus and minus two percent of their respective peak grain carbon. Red perimeters in (c) and (d) represent the areas greater than the 95$^{\text{th}}$ percentile of grain yields. (e) Vertical root carbon distributions averaged over growing seasons under default root structures (orange) and optimized root structures (red). The shaded red area in (e) represents the standard deviation related to the case of the optimized root traits.

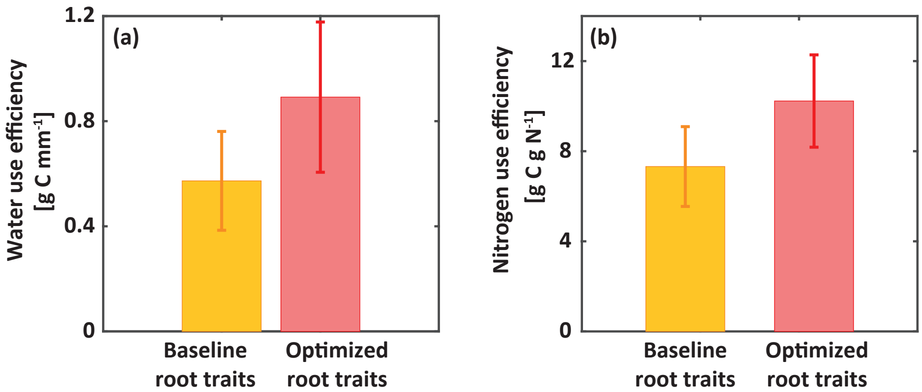

Figure 3: (a) Annual water use efficiency and (b) nitrogen use efficiency modeled from baseline and optimized root traits. The error bars represent the standard deviations over the 50 year simulations.

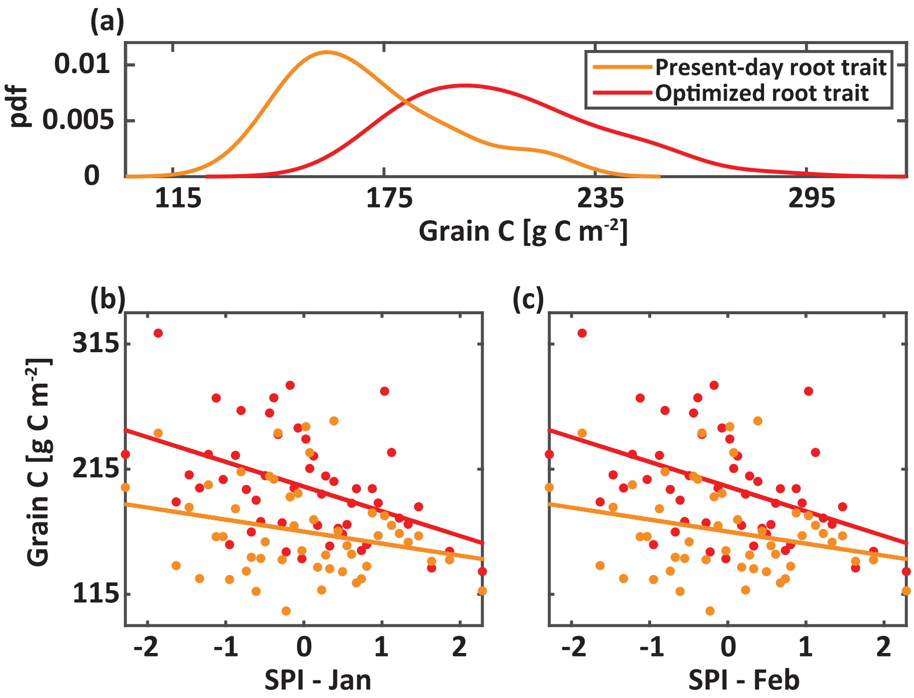

Figure 4: (a) Probability density functions (pdf) for grain carbon under baseline root traits (orange) and optimized root traits (red) over the study period. Pdf of averaged grain carbon modeled under optimized root traits (red; red area in Figure 2c, d). (b and c) Comparison between grain carbon and 3-month SPI (c) from November to January (SPI – Jan) and (d) from December to Feburary (SPI – Feb) with fitted linear regressions (solid lines).

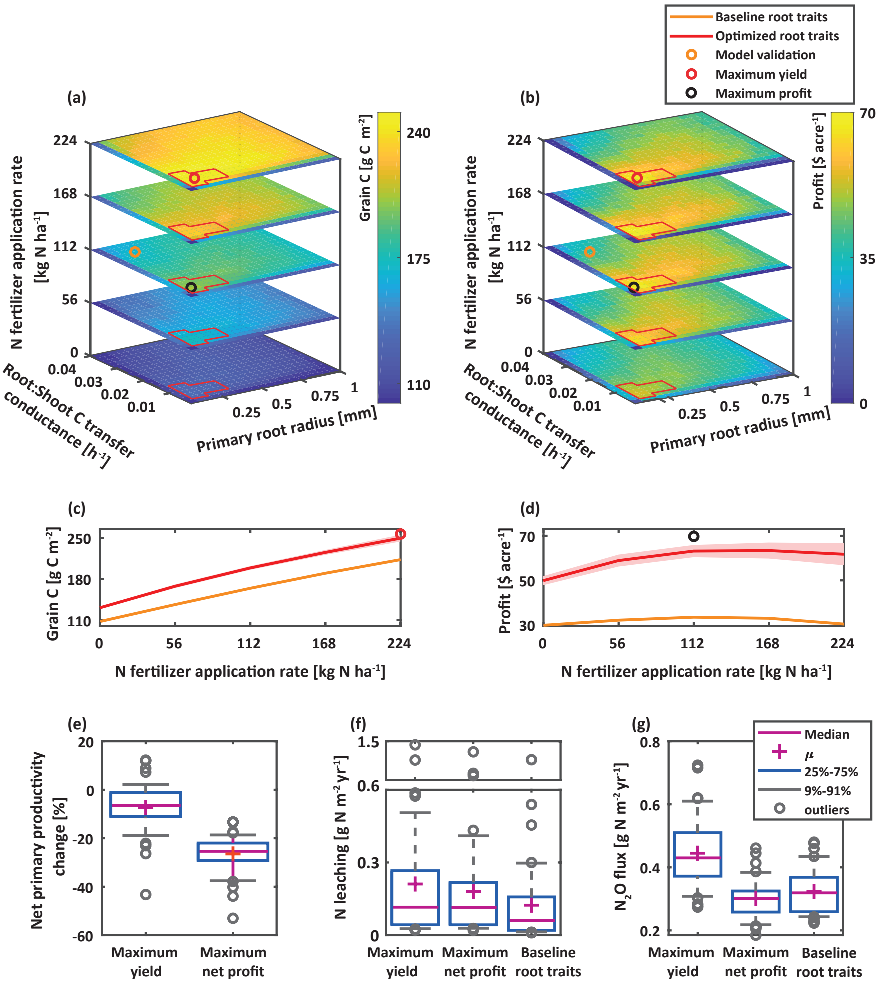

Figure 5: The top panels show how different nitrogen fertilizer application rates (z-axis) affect (a) grain carbon and (b) profit under the dependence of primary root radius (x-axis) and root:shoot carbon transfer conductance (y-axis). Each red perimeter in the different levels of fertilizer applications represents an area greater than the 95th percentile of their respective grain yields. The orange, red, and black circles are parameters and fertilizer rates from model validation, maximum yield, and maximum profit, respectively. (c and d) The impacts of nitrogen fertilizer application rate on (c) grain carbon and (d) profit under baseline root traits (orange) and optimized root traits (red). The shaded red areas in (c) and (d) are the standard deviations of grain carbon and profit, respectively. To assess the environmental consequences associated with the optimized root traits, (e), (f), and (g) show box plots for changes in net primary productivity, nitrogen leaching at the bottom of the soil column, and soil nitrous oxide (N_2O) fluxes, respectively, for the cases of maximum yield, maximum profit, and baseline root traits.

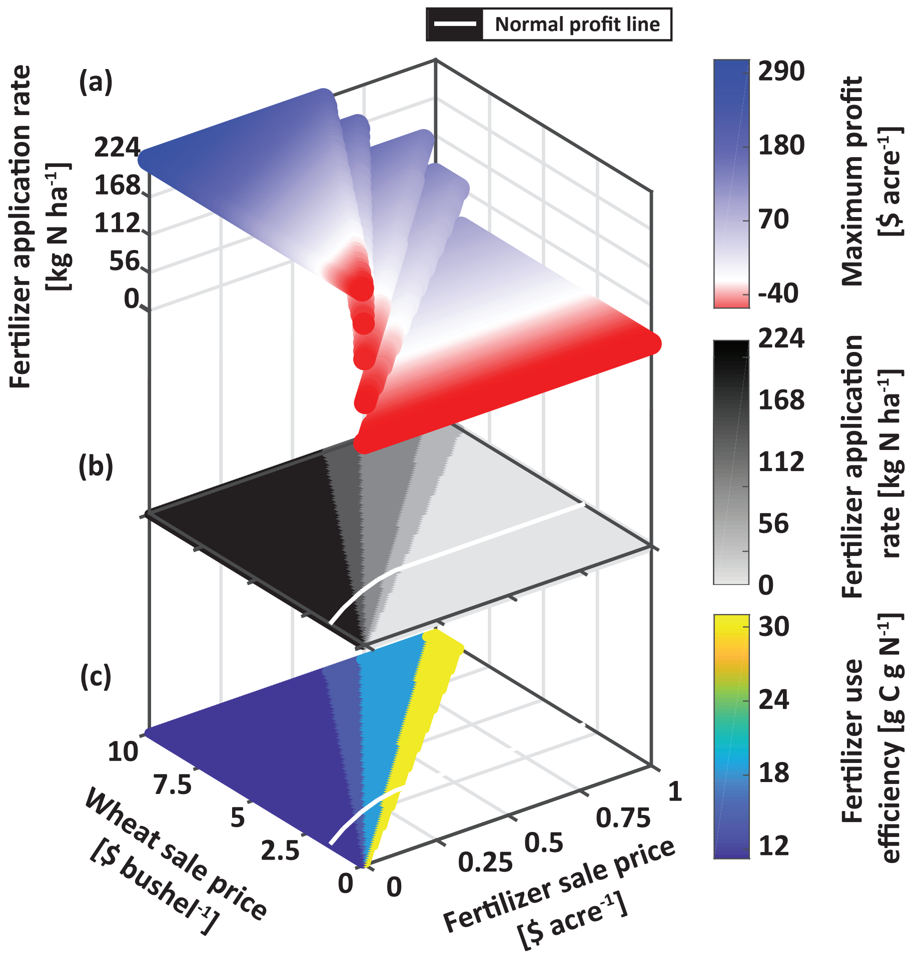

Figure 6: (a) The impacts of combined fertilizer sale price (x-axis), wheat sale price (y-axis), and fertilizer application rates (z-axis) on profit (color bar). The 2D projection of the fertilizer rates shown in z-axis in (a) is presented in (b) to enable visualization. (c) Fertilizer use efficiency, defined as yield per unit fertilizer input, associated with maximum profit under the different combinations of wheat and fertilizer sale prices. The white lines in (b) and (c) represent normal profits.

Table 1: Parameters used for the *ecosys* model. For parameters not listed in this table, see Grant (1998, 2013), and Grant et al. (2011) including online supplements.

Parameters and descriptions	Value
Horizontal mesh size, $\Delta x = \Delta y$ (m)	1
Vertical mesh size, Δz (m)	see foot note[a]
Overland flow	
Manning's coefficient ($m^{-1/3}$ h)	0.05[b]
Soil parameters	
Sand content (%)	24[c]
Clay content (%)	48[c]
Bulk density (Mg m^{-3})	1.39[c]
Field capacity (m^3 m^{-3})	0.36[d]
Wilting point (m^3 m^{-3})	0.16[d]
Saturated hydraulic conductivity (mm h^{-1})	8.8[e]
Wheat parameters	
Planting density (m^{-2})	350[c]
Rubisco carboxylation activity at 25°C (μmol g^{-1} s^{-1})	140[f]
Chlorophyll activity at 25°C (μmol g^{-1} s^{-1})	450[g]
Root porosity (m^3 m^{-3})	0.05[g]
Root radius (mm)	0.05-1.0†; 0.2*[j]
Root:Shoot carbon transfer conductance (h^{-1})	0.002-0.04†; 0.0375*[k]

[a] The vertical mesh sizes of 12 soil layers implemented are gradually increased as the depth is increased to the depth of 2 m.
[b]Chow (1959)
[c]Site observation
[d]Saxton and Rawls (2006)
[e]Clapp and Hornberger (1978)
[f]Perdomo et al. (2016)
[g]Farquhar et al. (1980)
[h]Wang. and Shangguan (2015)
[i]Striker et al. (2007)
[j]Munoz-Romero et al. (2010); Ward et al. (2011); Fricke et al. (2014); Colombi et al. (2017); Dal Cortivo et al. (2017) and Liu et al. (2018)
[k]Grant (1998)
†Parameter for the model validation.
*Parameter range for numerical optimization practices.

Appendix A

Description of water and nutrient uptake, five additional figures for the schematic diagram of *ecosys*, weather forcings, a time series of 3-month SPI, a relationship between grain carbon and 3-month SPI, and environmental consequences are presented in this Appendix to provide a more complete discussion of our results and to aid future readers.

A1 Water and nutrient uptake

Water uptake: Water uptake by plant roots is estimated as the difference between soil water potential and shoot water potential divided by the sum of (i) radial resistance to water transport from soil to surface of roots, (ii) radial resistance to water transport from surface to axis of roots, and (iii) axial resistance to water transport along axes of roots. To maintain a water balance between shoot, root, and soil systems, root water potential is estimated under the constraint that water fluxes out of soil layers are equal to the combined root water fluxes. To estimate the resistances, the cylindrical shapes of the primary and secondary roots are assumed based on their parametric root diameters and prognosed root lengths.

Nutrient uptake: Root nutrient uptake is iteratively estimated by letting (i) radial transport via advective and diffusive pathways between the soil solutions and root surfaces and (ii) active uptake by the surface, be the same (Grant., 1991; Grant & Heaney, 1997; Grant, 1998, 2013). Under the cylindrical root shape assumption, the radial transport (Q_p, g m^{-2} h^{-1}) is estimated as:

$$Q_p = Q_{up}[S]_s + 2\pi L_r D_e \frac{[S]_s - [S]_r}{\ln(d/r)} \tag{A1}$$

where Q_{up} is root water uptake (m3 m^{-2} h^{-1}); $[S]_s$ and $[S]_r$ are concentration of nutrient, such as ammonium, nitrate, and phosphorus in the soil (g g^{-1}) and at root surface (g g^{-1}), respectively; L_r is sum of root length (m^2 m^{-2}); D_e is effective dispersivity-diffusivity (m^2 h^{-1}); d is half distance between adjacent roots (m); r is effective root radius (m, hereinafter root radius). The active uptake (Q_a, g m^{-2} h^{-1}) is estimated as:

$$Q_a = \bar{Q}\frac{U_{O_2}}{\bar{U}_{O_2}} A_r \frac{[S]_r - [S]_m}{[S]_r - [S]_m + K_m} f_t f_m \tag{A2}$$

where $\bar{Q}$ is maximum $[S]_r$ at 25 °C and non-limiting $[S]_r$ conditions (g m^{-2} h^{-1}); U_{O_2} and $\bar{U}_{O_2}$ are O_2 uptake by roots under ambient O_2 and non-limiting O_2 conditions (g m^{-2} h^{-1}), respectively; A_r is root surface area (m^2 m^{-2}); $[S]_m$ is concentration of nutrient at root surface below which $[S]_r = 0$; K_m is Michaelis–Menten constant for nutrient uptake at root surface; f_t and f_m are temperature and nutrient inhibition of root nutrient uptake (−), respectively. Nutrients obtained from root systems influence leaf-level CO_2 fixation, and vice versa through phloem translocation of labile carbon, nitrogen, and phosphrous between shoots and roots (Grant, 1992). That is, a functional equilibrium between aboveground and belowground plant storage is achieved, enabling the adjustment of plant growth and metabolism to water- and nutrient-limited conditions.

A2 Figures

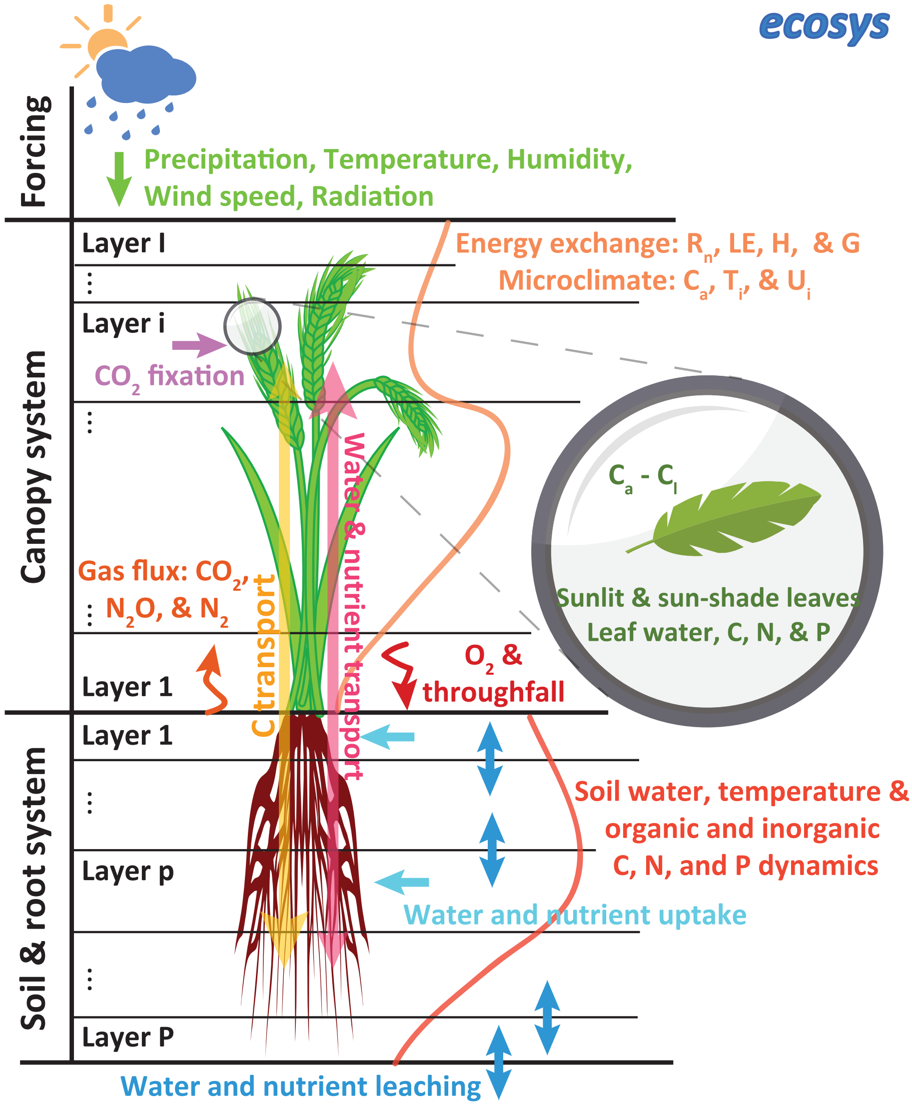

Figure A1: A schematic diagram showing *ecosys*, a coupled ecohydrological and biogeochemical model using multi-layer canopy and soil approaches. The forcings used in this model are precipitation, temperature, humidity, wind speed, and radiation. This model explicitly solves the vertical variations of canopy energy balances, such as net radiation (R_n), latent heat (LE), sensible heat (H), and ground heat (G) by considering canopy microclimate, such as canopy CO_2 concentration (C_a), canopy temperature (T_i), and canopy wind speed (U_i). The CO_2 fixation is controlled by differences between canopy and leaf CO_2 concentrations (C_l) and also affected by plant water, carbon (C), nitrogen (N), and phosphorus (P) availability. The growth of root influences its ability to obtain water and nutrient in the soil, which in turn affects aboveground plant dynamics through an exchange of water and nutrient between them. In the soil, water, temperature, and organic and inorganic C, N, and P dynamics are implemented, which directly affect overall plant performances through their effects on carboxylation and oxygenation. More details about this model including equations and parameters are described in the Supplement of Grant (2013).

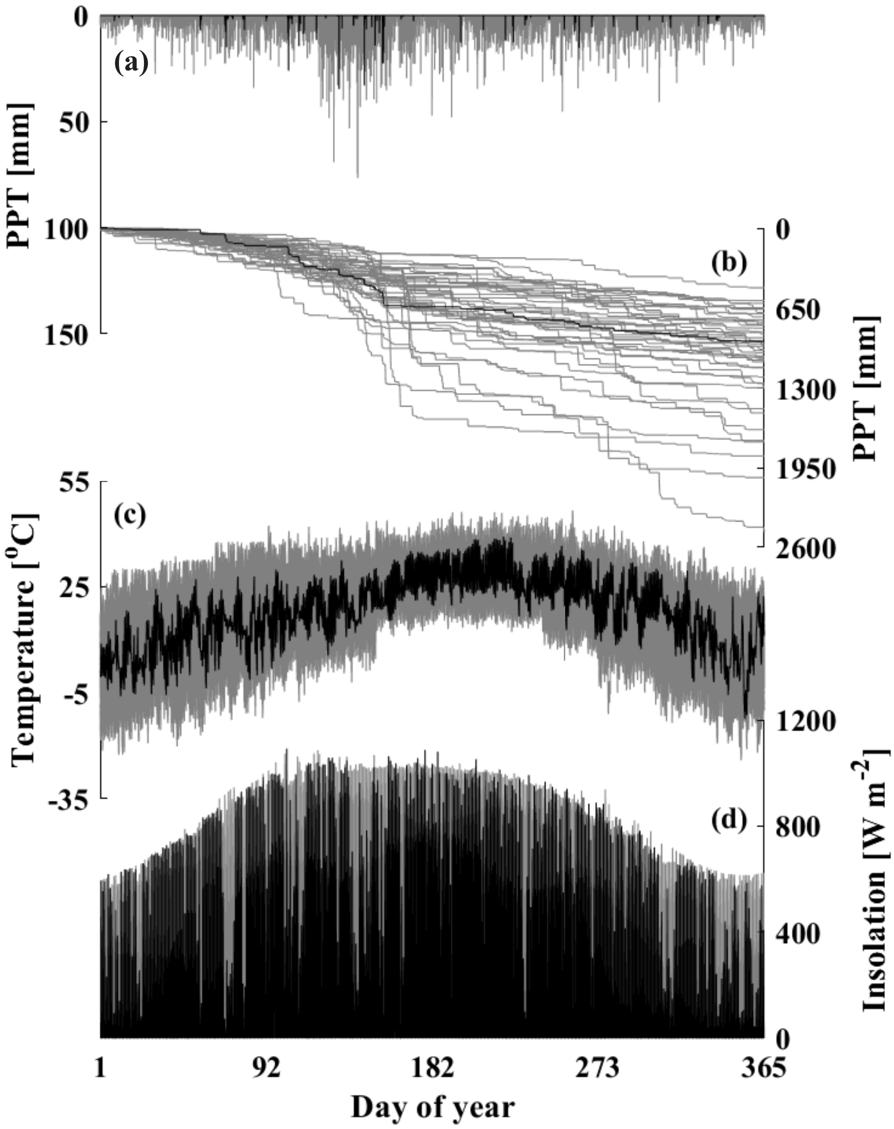

Figure A2: Observed weather data in 2017 (black) are overlaid on the ensemble of stochastically generated weather forcings (gray) generated using a weather generator (Fatichi et al., 2010) based on the observed weather data from 1994 to 2018. (a) Precipitation, (b) Cumulative precipitation, (c) Air temperature, and (d) Solar radiation.

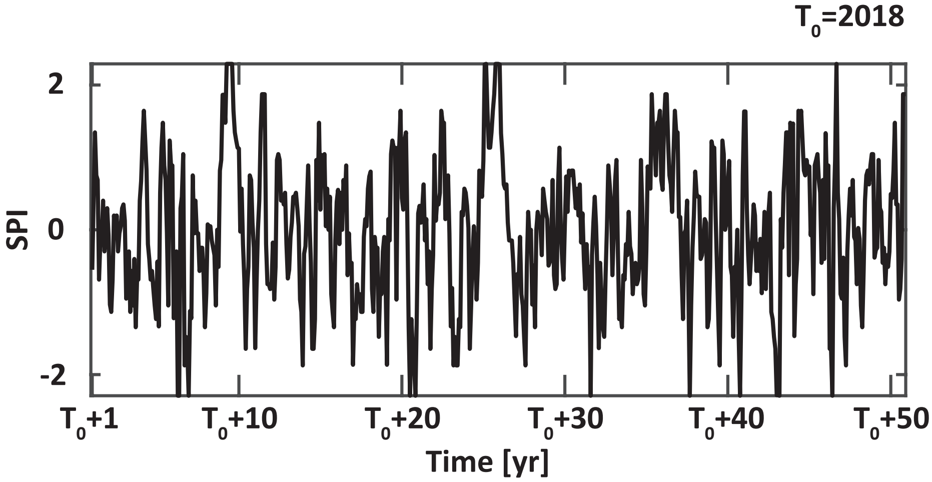

Figure A3: A time series of 3-month standardized precipitation index (SPI) over the 50 years after T_0=2018.

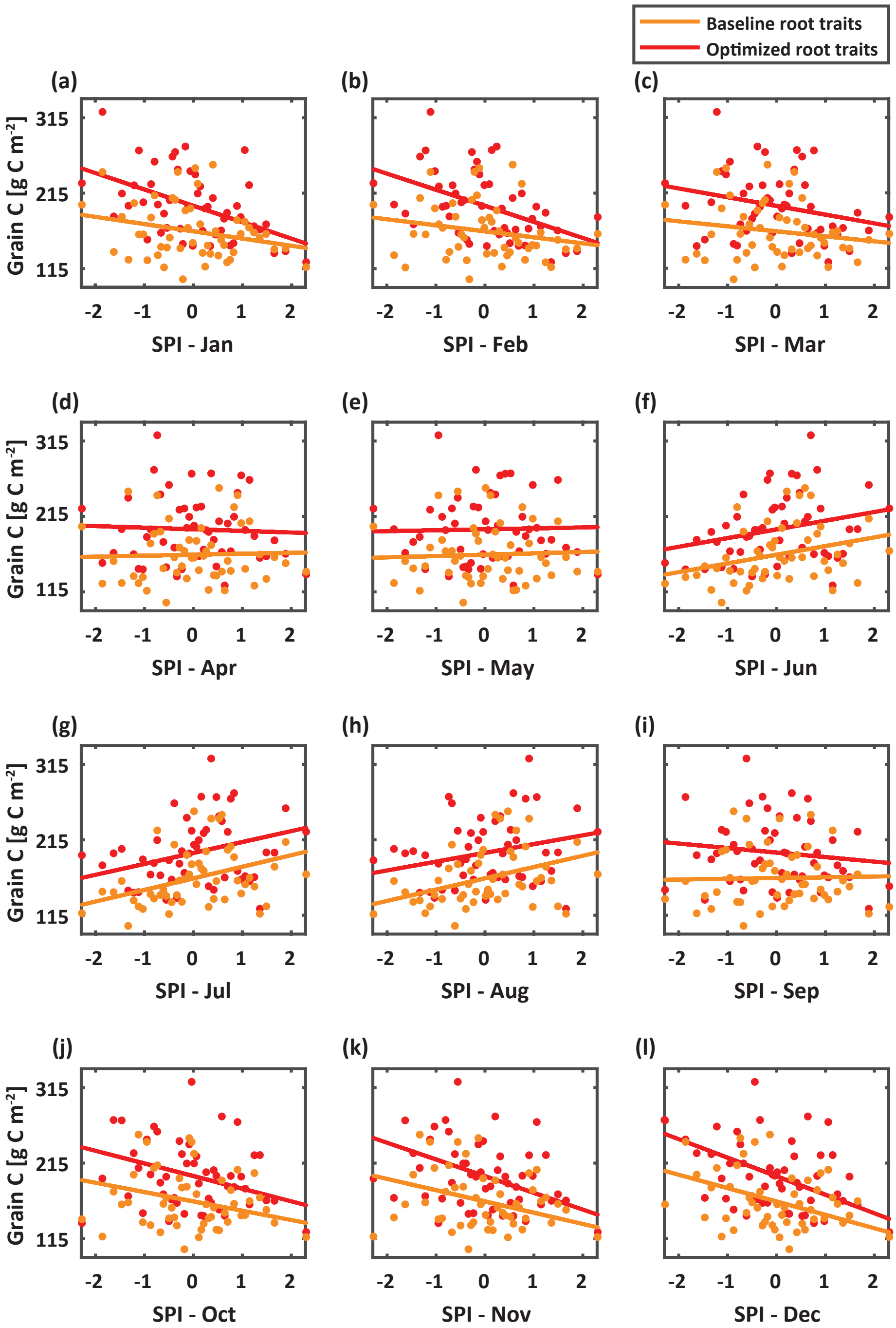

Figure A4: To explore the impacts of precipitation variability on winter wheat yields, (a to l) comparisons between grain carbon and 3-month SPI with fitted linear regressions as presented in solid lines. For example, 3-month SPI from November to January is denoted as SPI-Jan. The orange and red colors represent the dynamics pertaining to baseline, and optimized root traits, respectively.

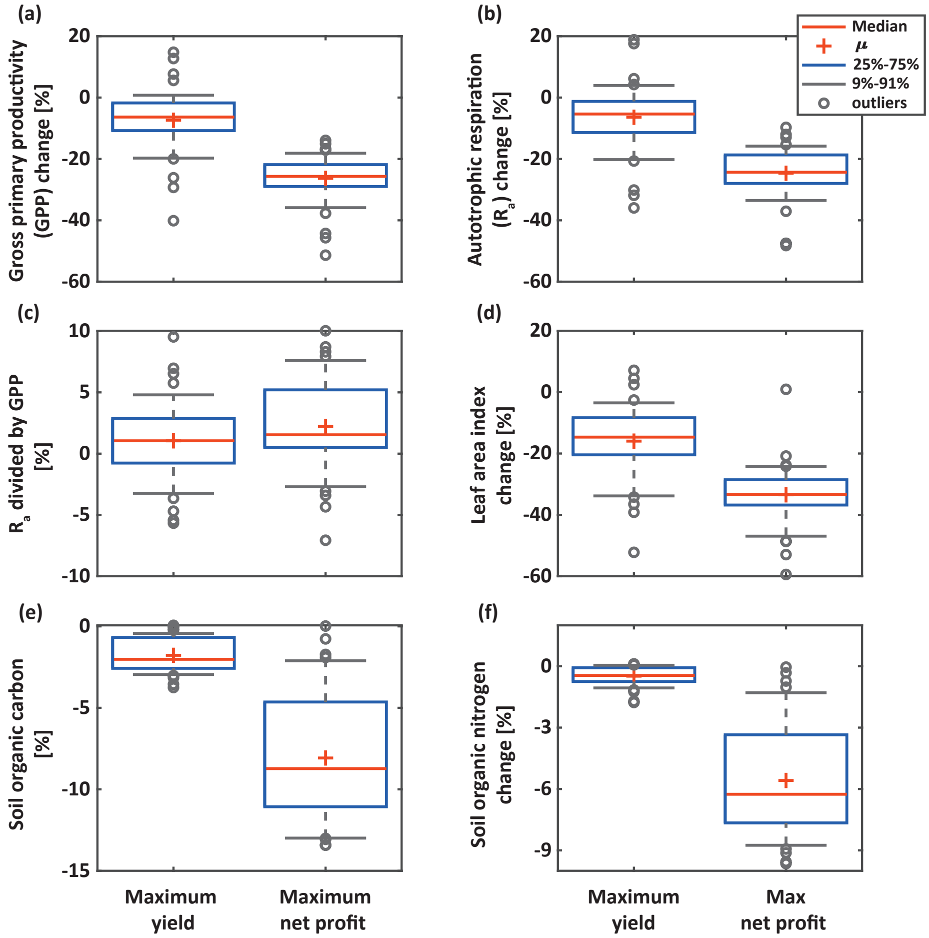

Figure A5: To assess the environmental consequences associated with the optimized root traits, box plots were used to present changes in (a) gross primary productivity (GPP), (b) autotrophic respiration (R_a), (c) R_a divided by GPP, (d) leaf area index, (e) soil organic carbon, and (f) soil organic nitrogen for the case of maximum yield (left) and maximum profit (right).

Acknowledgments

This work was supported the National Research Foundation of Korea (NRF) grant funded by the Korea government (MSIT) (No. 2021R1C1C1004801) and the U.S. Department of Energy grant under Contract No. 16/CJ000/04/08 as part of the Tomographic Electrical Rhizosphere Imaging (TERI) proejct. All of the numerical information in the figures is produced by solving the equations in the Supplement of (Grant, 2013). The weather data used in this study are obtained from Weather Underground (`https://www.wunderground.com/weather/us/ok/ardmore`) and the National Solar Radiation Database (`https://maps.nrel.gov/nsrdb-viewer`) and the winter wheat yield data used in this study are obtained from the National Agricultural Statistics Service (`https://quickstats.nass.usda.gov/%236F8CB0F4-B04E-3055-BE27-0E765544EEA3`).

References

Ao, J., Fu, J., Tian, J., Yan, X., & Liao, H. (2010). Genetic variability for root morph-architecture traits and root growth dynamics as related to phosphorus efficiency in soybean. *Functional Plant Biology*, *37*, 304–312. doi: 10.1071/FP09215

Araus, J. L., Reynolds, M., & Acevedo, E. (1993). Leaf posture, grain yield, growth, leaf structure, and carbon isotope discrimination in wheat. *Crop Science*, *33*, 1273–1279. doi: 10.2135/cropsci1993.0011183X003300060032x

Aziz, M. M., Palta, J. A., Siddique, K. H. M., & Sadras, V. O. (2017). Five decades of selection for yield reduced root length density and increased nitrogen uptake per unit root length in Australian wheat varieties. *Plant and Soil*, *413*, 181–192. doi: 10.1007/s11104-016-3059-y

Bajzelj, B., Richards, K. S., Allwood, J. M., Smith, P., Dennis, J. S., Curmi, E., & Gilligan, C. A. (2014). Importance of food-demand management for climate mitigation. *Nature Climate Change*, *4*, 924–929. doi: 10.1038/NCLIMATE2353

Braun, H. J., Atlin, G., & Payne, T. (2000). *Multi-location testing as a tool to identify plant response to global climate change, in climate change and crop production* (M. P. Reynolds, Ed.). CABI: Wallingford, UK. doi: 10.1079/9781845936334.0115

Brouwer, R. (1962). Nutritive influences on the distribution of dry matter in the plant. *Neth. J. agric. Sei.*, *10*, 399–408.

Brugge, R., & Thornley, J. H. M. (1985). A growth model of root mass and vertical distribution dependent on carbon substrate from photosynthesis and with non-limiting soil conditions. *Annals of Botany*, *55*, 563–577. doi: 10.1093/oxfordjournals.aob.a086931

Chow, V. T. (1959). *Open-channel hydraulics.* McGraw-Hill, New York, USA.

Ciampitti, I., & Vyn, T. (2014). Understanding global and historical nutrient use efficiencies for closing maize yield gaps. *Agronomy Journal*, *106*, 2107–2117. doi: 10.2134/agronj14.0025

Clapp, R. B., & Hornberger, G. N. (1978). Empirical equations for some soil hydraulic properties. *Water Resour. Res.*, *14*, 601–604. doi: 10.1029/WR014i004p00601

Colombi, T., Kirchgessner, N., Walter, A., & Keller, T. (2017). Root tip shape governs root elongation rate under increased soil strength. *Plant Physiol.*, *174*, 2289–2301. doi: 10.1104/pp.17.00357

Cormier, F., Foulkes, J., Hirel, B., Gouache, D., Moenne-Loccoz, Y., & Gouis, J. L. (2016). Breeding for increased nitrogen-use efficiency: a review for wheat (*T. aestivum* L.). *Plant Breed.*, *135*, 255–278. doi: 10.1111/pbr.12371

Dal Cortivo, C., Barion, G., Visioli, G., Mattarozzi, M., Mosca, G., & Vamerali, T. (2017). Increased root growth and nitrogen accumulation in common wheat following PGPR inoculation: Assessment of plant-microbe

interactions by ESEM. *Agric Ecosyst Environ.*, *247*, 396–408. doi: 10.1080/17429145.2018.1432770
DeVuyst, E. A. (2012). *Canola budgets comparison to wheat 2012.* Retrieved from `http://canola.okstate.edu/cropproduction/economics/`
Doi, R., & Pitiwut, S. (2014). From maximization to optimization: a paradigm shift in rice production in thailand to improve overall quality of life of stakeholders. *The Scientific World Journal*, *2014*, 604291. doi: 10.1155/2014/604291
Drewry, D. T., Kumar, P., & Long, S. P. (2014). Simultaneous improvement in productivity, water use, and albedo through crop structural modification. *Global Change Biology*, *20*, 1955–1967. doi: 10.1111/gcb.12567
Dunbabin, V., Diggle, A., & Rengel, Z. (2003). Is there an optimal root architecture for nitrate capture in leaching environments? *Plant Cell Environ.*, *26*, 835–844. doi: 10.1046/j.1365-3040.2003.01015.x
Eddy, A. (1982). *A rainfall climatology for Oklahoma–Operational weather modification* (Tech. Rep. Nos. 5, 120 p.) Oklahoma Climatological Survey.
Edgerton, M. D. (2009). Increasing crop productivity to meet global needs for feed, food, and fuel. *Plant Physiol*, *149*, 7–13. doi: 10.1104/pp.108.130195
Erisman, J. W., Sutton, M. A., Galloway, J., Klimont, Z., & Winiwarter, W. (2008). How a century of ammonia synthesis changed the world. *Nature Geoscience*, *1*, 636–639. doi: 10.1038/ngeo325
Fageria, N. K., dos Santos, A. B., & Coelho, A. M. (2011). Growth, yield and yield components of lowland rice as influenced by ammonium sulfate and urea fertilization. *Journal of Plant Nutrition*, *34*, 371–386. doi: 10.1080/01904167.2011.536879
Fan, M., Shen, J., Yuan, L., Jiang, R., Chen, X., Davies, W. J., & Zhang, F. (2012). Improving crop productivity and resource use efficiency to ensure food security and environmental quality in China. *Journal of Experimental Botany*, *63*, 13–24. doi: 10.1093/jxb/err248
FAO. (2009). *Global agriculture towards 2050.* FAO, Rome, Italy.
Farquhar, G. D., von Caemmerer, S., & Berry, J. A. (1980). A biochemical model of photosynthetic co_2 assimilation in leaves of C3 species. *Planta*, *49*, 78–90. doi: 10.1007/BF00386231
Fatichi, S., Ivanov, V. Y., & Caporali, E. (2010). Simulation of future climate scenarios with a weather generator. *Adv. Water Resour.*, *34*, 448–467. doi: 10.1016/j.advwatres.2010.12.013
Feller, C., Favre, P., Janka, A., Zeeman, S. C., Gabriel, J.-P., & Reinhardt, D. (2015). Mathematical modeling of the dynamics of shoot-root interactions and resource partitioning in plant growth. *PLoS ONE*, *19*, e0127905. doi: 10.1371/journal.pone.0127905
Foley, J. A., Ramankutty, N., Brauman, K. A., Cassidy, E. S., Gerber, J. S., Johnston, M., ... Zaks, D. P. M. (2011). Solutions for a cultivated planet. *Nature*, *478*, 337–342. doi: 10.1038/nature10452
Foulkes, M. J., Slafer, G. A., Davies, W. J., Berry, P. M., Sylvester-Bradley, R., Martre, P., ... Reynolds, M. P. (2011). Raising yield potential of wheat. III. optimizing partitioning to grain while maintaining lodging resistance. *J. Exp. Bot.*, *62*, 469–486. doi: 10.1093/jxb/erq300
Fricke, W., Bijanzadeh, E., Emam, Y., & Knipfer, T. (2014). Root hydraulics in salt-stressed wheat. *Functional Plant Biology*, *41*, 366–378. doi: 10.1071/fp13219
Frieler, K., Schauberger, B., Arneth, A., Balkovic, J., Chryssanthacopoulos, J., Deryng, D., ... Levermann, A. (2017). Understanding the weather signal in national crop-yield variability. *Earth's Future*, *5*, 605–616. doi: 10.1002/2016EF000525
Gandorfer, M., & Rajsic, P. (2008). Modeling economic optimum 0itrogen rates for winter wheat when inputs affect yield and output-price. *Agricultural Eco-*

nomics Review, *9*, 51–64.
Gardner, J. B., & Drinkwater, L. E. (2009). The fate of nitrogen in grain cropping systems: a meta-analysis of 15N field experiments. *Ecol Appl.*, *19*, 2167–2184. doi: 0.1890/08-1122.1
Geng, J., Sun, Y., Zhang, M., Li, C., Yang, Y., Liu, Z., & Li, S. (2015). Long-term effects of controlled release urea application on crop yields and soil fertility under rice-oilseed rape rotation system. *Field Crops Res.*, *184*, 65–73. doi: 10.1016/j.fcr.2015.09.003
Gerland, P., Raftery, A. E., Sevcikova, H., Li, N., Gu, D., Spoorenberg, T., ... Wilmoth, J. (2014). World population stabilization unlikely this century. *Science*, *346*, 234–237. doi: 10.1126/science.1257469
Gill, B. S., Appels, R., Botha-Oberholster, A.-M., Buell, C. R., Bennetzen, J. L., Chalhoub, B., ... Sasaki, T. (2004). A workshop report on wheat genome sequencing: International genome research on wheat consortium. *Genetics*, *168*, 1087–1096. doi: 10.1534/genetics.104.034769
Godfray, H. C. J., Beddington, J. R., Crute, I. R., Haddad, L., Lawrence, D., Muir, J. F., ... Toulmin, C. (2010). Food security: The challenge of feeding 9 billion people. *Science*, *327*, 812–818. doi: 10.1126/science.1185383
Good, A. G., & Beatty, P. H. (2011). Fertilizing nature: A tragedy of excess in the commons. *PLoS Biol*, *9(8)*, e1001124. doi: 10.1371/journal.pbio.1001124
Goulding, K., Jarvis, S., & Whitmore, A. (2008). Optimizing nutrient management for farm systems. *Philos Trans R Soc Lond B Biol Sci.*, *363*, 667–680. doi: 10.1098/rstb.2007.2177
Grant, R. (1992). Simulation of carbon dioxide and water deficit effects upon photosynthesis of soybean leaves with testing from growth chamber studies. *Crop Sci.*, *32*, 1313–1321. doi: 10.1007/BF00779170
Grant, R. (2013). Modelling changes in nitrogen cycling to sustain increases in forest productivity under elevated atmospheric CO_2 and contrasting site conditions. *Biogeosciences*, *10*, 7703-7721. doi: 10.5194/bg-10-7703-2013
Grant, R., Wall, G. W., Kimball, B. A., Frumau, K. F. A., Pinter Jr, P. J., Hunsaker, D. J., & Lamorte, R. L. (1999). Crop water relations under different CO_2 and irrigation: Testing of ecosys with the free air CO_2 enrichment (FACE) experiment. *Agricultural and Forest Meteorology*, *95*, 27–51. doi: 10.1016/S0168-1923(99)00017-9
Grant., R. F. (1991). The distribution of water and nitrogen in the soil-crop system: A simulation study with validation from a winter wheat field trial. *Fertilizer research*, *27*, 199–213. doi: 10.1007/BF01051128
Grant, R. F. (1993a). Simulation model of soil compaction and root growth. II. model testing. *Plant and Soil*, *150*, 15–24. doi: 10.1007/BF00779171
Grant, R. F. (1993b). Simulation model of soil compaction and root growth. I. model development. *Plant and Soil*, *150*, 1–14. doi: 10.1007/BF00779170
Grant, R. F. (1998). Simulation in ecosys of root growth response to contrasting soil water and nitrogen. *Ecological Modelling*, *107*, 237–264. doi: 10.1016/S0304-3800(97)00221-4
Grant, R. F., & Heaney, D. (1997). Inorganic phosphorus transformations and transport in soils: mathematical modelling in ecosys. *oil Sci. Soc. Am. J.*, *61*, 752–764. doi: 10.2136/sssaj1997.03615995006100030008x
Grant, R. F., Juna, N. G., & McGill, W. B. (1993). Simulation of carbon and nitrogen transformations in soil: Mineerlization. *Soil Biol. Biochem.*, *25*, 1317–1329. doi: 10.1016/0038-0717(93)90046-E
Grant, R. F., Kimball, B. A., Conley, M. M., White, J. W., Wall, G. W., & Ottman, M. J. (2011). Controlled warming effects on wheat growth and yield: Field measurements and modeling. *Agronomy Journal*, *103*, 1742–1754. doi: 10.2134/agronj2011.0158
Grant, R. F., Kimball, B. A., Pinter Jr., P. J., Wall, G. W., Garcia, R. L., La Morte,

R. L., & Hunsaker, D. J. (1995). Carbon dioxide effects on crop energy balance: Testing *ecosys* with a Free-Air CO_2 Enrichment (FACE) experiment. *Agron. J.*, *87*, 446–457. doi: 10.2134/agronj1995.00021962008700030010x

Guttman, N. B. (1998). Comparing the palmer drought index and the standardized precipitation index. *J. Amer. Water Resour. Assoc.*, *34*, 113–121. doi: 10.1111/j.1752-1688.1998.tb05964.x.

Hao, Z., & AghaKouchak, A. (2014). A nonparametric multivariate multi-index drought monitoring framework. *Journal of Hydrometeorology*, *15*, 89–101. doi: 10.1175/JHM-D-12-0160.1

Herder, G. D., Van Isterdael, G., Beeckman, T., & De Smet, I. (2010). The roots of a new green revolution. *Trends Plant Sci.*, *15*, 600–607. doi: 10.1016/j.tplants.2010.08.009

Hulme, M. F., Vickery, J. A., Green, R. E., Phalan, B., Chamberlain, D. E., Pomeroy, D. E., … Atkinson, P. W. (2013). Conserving the birds of Uganda's banana–coffee arc: Land sparing and land sharing compared. *PLOS ONE*, *8*, e54597. doi: 10.1371/journal.pone.0054597

Islam, M. T., Islam, A. F. M. S., & Uddin, M. S. (2019). Physiological growth indices of maize (*Zea mays* L.) genotypes in sylhet. *bioRxiv*. doi: 10.1101/518993

Islam., S., & Talukdar, B. (2014). Crop yield optimization using genetic algorithm with the CROPWAT model as a decision support system. *Internat. J. Agric. Engg.*, *7*, 7–14.

Ju, C., Buresh, R. J., Wang, Z., Zhang, H., Liu, L., Yang, J., & Zhang, J. (2015). Root and shoot traits for rice varieties with higher grain yield andhigher nitrogen use efficiency at lower nitrogen rates application. *Field Crops Research*, *175*, 47–55. doi: 10.1016/j.fcr.2015.02.007

Karp, A., Edwards, K. J., Bruford, M., Funk, S., Vosman, B., Morgante, M., … Hewitt, G. M. (1997). Molecular technologies for biodiversity evaluation: Opportunities and challenges. *Nature Biotechnology*, *15*, 625–628. doi: 10.1038/nbt0797-625

Kihara, J., Nziguheba, G., Zingore, S., Coulibaly, A., Esilaba, A., Kabambe, V., … Huising, J. (2016). Understanding variability in crop response to fertilizer and amendments in sub-Saharan Africa. *Agriculture, Ecosystems & Environment*, *229*, 1–12. doi: 10.1016/j.agee.2016.05.012

Kocyigit, R., & Rice, C. W. (2004). Carbon dynamics in tallgrass prairie and wheat ecosystems. *Turkish Journal of Agriculture and Forestry*, *28*, 141–153.

Koziel, M. G., Beland, G. L., Bowman, C., Carozzi, N. B., Crenshaw, R., Crossland, L., … Evola, S. V. (1993). Field performance of elite transgenic maize plants expressing an insecticidal protein derived from bacillus thuringiensis. *Bio/Technologyvolume*, *11*, 194–200. doi: 10.1038/nbt0293-194

Li, H., Sivapalan, M., Tian, F., & Liu, D. (2010). Water and nutrient balances in a large tile-drained agricultural catchment: a distributed modeling study. *Hydrol. Earth Syst. Sci.*, *14*, 2259–2275. doi: 10.5194/hess-14-2259-2010

Li, X., Zeng, R., & Liao, H. (2016). Improving crop nutrient efficiency through root architecture modifications. *J Integr Plant Biol.*, *58*, 193–202. doi: 10.1111/jipb.12434

Lin, B. B. (2011). Resilience in agriculture through crop diversification: Adaptive management for environmental change. *BioScience*, *61*, 183–193. doi: 10.1525/bio.2011.61.3.4

Linquist, B. A., Liu, L., van Kessel, C., & van Groenigen, K. J. (2013). Enhanced efficiency nitrogen fertilizers for rice systems: Meta-analysis of yield and nitrogen uptake. *Field Crops Research*, *154*, 246–254. doi: 10.1016/j.fcr.2013.08.014

Liu, X., Dong, X., Xue, Q., Leskovar, D. I., Jifon, J., Butnor, J. R., & Marek, T. (2018). Ground penetrating radar (GPR) detects fine roots of agricultural

crops in the field. *Plant Soil*, *423*, 517–531. doi: 10.1007/s11104-017-3531-3
Lobell, D. B., Burke, M. B., Tebaldi, C., Mastrandrea, M. D., Falcon, W. P., & Naylor, R. L. (2008). Prioritizing climate change adaptation needs for food security in 2030. *Science*, *319*, 607–610. doi: 10.1126/science.1152339
Lobell, D. B., Schlenker, W., & Costa-Roberts, J. (2011). Climate trends and global crop production since 1980. *Science*, *333*, 616–620. doi: 10.1126/science.1204531
Lonbani, M., & Arzani, A. (2011). Morpho-physiological traits associated with terminal droughtstress tolerance in triticale and wheat. *Agronomy Research*, *9*, 315–329.
Long, S. P., Humphries, S., & Falkowski, P. G. (1994). Photoinhibition of photosynthesis in nature. *Annu. Rev. Plant Biol.*, *45*, 633–662. doi: 10.1146/annurev.pp.45.060194.003221
Long, S. P., Zhu, X. G., Naidu, S. L., & Ort, D. R. (2006). Can improvement in photosynthesis increase crop yields? *Plant Cell Environ*, *29*, 315–330. doi: 10.1111/j.1365-3040.2005.01493.x
Lopes, M. S., Royo, C., Alvaro, F., Sanchez-Garcia, M., Ozer, E., Ozdemir, F., … Pequeno, D. (2018). Optimizing winter wheat resilience to climate change in rain fed crop systems of Turkey and Iran. *Front. Plant Sci.*, *9*, 563. doi: 10.3389/fpls.2018.00563
Lu, C., & Tian, H. (2017). Global nitrogen and phosphorus fertilizer use for agriculture production in the past half century: shifted hot spots and nutrient imbalance. *Earth Syst. Sci. Data*, *9*, 181–192. doi: 10.5194/essd-9-181-2017
Lynch, J. P. (2018). Rightsizing root phenotypes for drought resistance. *J Exp Bot. Jun*, *69*, 3279–3292. doi: 10.1093/jxb/ery048
Macrotrends. (2019). Retrieved from `https://www.macrotrends.net/2534/wheat-prices-historical-chart-data`
Malve, S. H., Rao, P., & Dhake, A. (2016). Evaluation of water production function and optimization of water for winter wheat (*Triticum aestivum* l.) under drip irrigation. *American-Eurasian J. Agric. & Environ. Sci.*, *16*, 1389–1398. doi: 10.5829/idosi.aejaes.2016.16.7.12970
Mekonnen, Z. A., Riley, W. J., & Grant, R. F. (2018). Accelerated nutrient cycling and increased light competition will lead to 21^{st} century shrub expansion in North American Arctic tundra. *Journal of Geophysical Research: Biogeosciences,*, *123*, 1683–1701. doi: 10.1029/2017JG004319
Merrill, A. L., & Watt, B. K. (1973). *Energy value of foods: Basis and derivation.* US Department of Agriculture, Agricultural Research Service, Washington DC.
Miflin, B. (2000). Crop improvement in the 21^{st} century. *Journal of Experimental Botany*, *51*, 1–8. doi: 10.1093/jexbot/51.342.1
Mueller, N. D., Gerber, J. S., Johnston, M., Ray, D. K., Ramankutty, N., & Foley, J. A. (2013). Closing yield gaps through nutrient and water management. *Nature*, *490*, 254–257. doi: 10.1038/nature11420
Munoz-Romero, V., Benitez-Vega, J., Lopez-Bellido, L., & Lopez-Bellido, R. J. (2010). Monitoring wheat root development in a rainfed vertisol: Tillage effect. *European Journal of Agronomy*, *33*, 182–187. doi: 10.1016/j.eja.2010.05.004
Natarajan, M., & Willey, R. W. (1996). The effects of water stress on yields advantages of intercropping systems. *Field Crop Res*, *13*, 117–131. doi: 10.1016/0378-4290(86)90015-8
Ortez, O. A., Salvagiotti, F., Enrico, J. M., Prasad, P. V. V., Armstrong, P., & Ciampitti, I. A. (2018). Exploring nitrogen limitation for historical and modern soybean genotypes. *Agronomy Journal*, *110*, 2080–2090. doi: 10.2134/agronj2018.04.0271
Oyangi, A. (1994). Gravitropic response growth angle and vertical distribution of roots of wheat. *Plant and Soil*, *165*, 323–326. doi: 10.1007/BF00008076

Pannell, D. J. (1999). Social and economic challenges in the development of complex farming systems. *Agroforestry Systems*, *45*, 393–409. doi: 10.1023/A:1006282614791

Perdomo, J. A., Carmo-Silva, E., Hermida-Carrera, C., Flexas, J., & Galmes, J. (2016). Acclimation of biochemical and diffusive components of photosynthesis in rice, wheat, and maize to heat and water deficit: Implications for modeling photosynthesis. *Front. PlantSci.*, *7*, 1719. doi: 10.3389/fpls.2016.01719

Phalan, B., Balmford, A., E.Green, R., & Scharlemannc, J. P. (2011). Minimising the harm to biodiversity of producing more food globally. *Food Policy*, *36*, S62–S71. doi: 10.1016/j.foodpol.2010.11.008

Population Division of United Nations. (2017). *World population prospects: The 2017 revision.* United Nations: New York, NY, USA.

Porkka, M., Guillaume, J. H. A., Siebert, S., Schaphoff, S., & Kummu, M. (2017). The use of food imports to overcome local limits to growth. *Earth's Future*, *5*, 393–407. doi: 10.1002/2016EF000477

Prasad, P. V. V., Satyanarayana, V., Murthy, V. R. K., & Boote, K. J. (2002). Maximizing yields in rice–groundnut cropping sequence through integrated nutrient management. *Field Crops Research*. doi: 10.1016/S0378-4290(01)00214-3

Radcliffe, D. E., Reid, D. K., Blomback, K., Bolster, C. H., Collick, A. S., Easton, Z. M., ... Smith, D. R. (2015). Applicability of models to predict phosphorus losses in drained fields: a review. *J Environ Qual.*, *44(2)*, 614-628. doi: 10.2134/jeq2014.05.0220

Raun, W. R., & Johnson, G. V. (1999). Improving nitrogen use efficiency for cereal production. *Agronomy journal*, *91*, 357–363. doi: 10.2134/agronj1999.00021962009100030001x

Ray, D. K., Mueller, N. D., West, P. C., & Foley, J. A. (2013). Yield trends are insufficient to double global crop production by 2050. *Plos One*, *8*, e66428. doi: 10.1371/journal.pone.0066428

Rebetzke, G. J., Botwright, T. L., Moore, C. S., Richards, R. A., & Condon, A. G. (2004). Genotypic variation in specific leaf area for genetic improvement of early vigour in wheat. *Field Crops Research*, *88*, 179–189. doi: 10.1016/j.fcr.2004.01.007

Richards. (1931). Capillary conduction of liquids in porous mediums. *Physics*, *1*, 318–333. doi: 10.1063/1.1745010

Richards, D. (1978). Root-shoot interactions: Functional equilibria for nutrient uptake in peach (*Prunuspersica* l. batsch.). *Annals of Botany*, *42*, 1039–1943. doi: 10.1093/oxfordjournals.aob.a085543

Richards., R. A. (2000). Selectable traits to increase crop photosynthesis and yield of grain crops. *Journal of Experimental Botany*, *51*, 447–458. doi: 10.1093/jexbot/51.suppl_1.447

Rosegrant, M. W., & Agcaoili, M. (2010). *Global food demand, supply and price prospects to 2010.* Washington DC, USAInternational Food Policy Research Institute.

Saxton, K. E., & Rawls, W. J. (2006). Soil water characteristic estimates by texture and organic matter for hydrologic solutions. *Soil Science Society of America Journal.*, *70*, 1569–1578. doi: 10.1.1.452.9733

Sieling, K., Bottcher, U., & Kage, H. (2016). Dry matter partitioning and canopy traits in wheat and barley under varying N supply. *European Journal of Agronomy*, *74*, 1–8. doi: 10.1016/j.eja.2015.11.022

Sinclair, T. R., & Rufty, T. W. (2012). Nitrogen and water resources commonly limit crop yield increases, not necessarily plant genetics. *Global Food Security*, *1*, 94–98. doi: 10.1016/j.gfs.2012.07.001

Sinha, E., Michalak, A. M., & Balaji, V. (2017). Eutrophication will increase during the 21st century as a result of precipitation changes. *Science*, *357*, 405–408. doi: 10.1126/science.aan2409

Spitzer, B., Mende, C., Menner, M., & Luck, T. (1996). Determination of the carbon content of biomass–a prerequisite to estimate the complete biodegradation of polymers. *Journal of environmental polymer degradation*, *4*, 157–171. doi: 10.1007/BF02067450

Srinivasan, V., Kumar, P., & Long, S. P. (2016). Decreasing, not increasing, leaf area will raise crop yields under global atmospheric change. *Global Change Biology*, *23*, 1626–1635. doi: 10.1111/gcb.13526

Striker, G. G., Insausti, P., Grimoldi, A. A., & Vega, A. (2007). Trade-off between root porosity and mechanical strength in species with different types of aerenchyma. *Plant Cell Environ.*, *30*, 580–589. doi: 10.1111/j.1365-3040.2007.01639.x

Tilman, D., Balzer, C., Hill, J., & Befort, B. L. (2011). Global food demand and the sustainable intensification of agriculture. *Proc Natl Acad Sci*, *108*, 20260–20264. doi: 10.1073/pnas.1116437108

Tripathi, S., Chander, S., Meena, R. . M. w. y. t. i. u. o. f. m., & fertilizers. (2016). Maximizing wheat yield through integrated use of farmyard manure and fertilizers. *SAARC Journal of Agriculture*, *14*, 103-110. doi: 10.3329/sja.v14i1.29580

USDA. (2019a). *Fertilizer use and price.* Retrieved from `https://www.ers.usda.gov/data-products/fertilizer-use-and-price.aspx`

USDA. (2019b). *Wheat data.* Retrieved from `https://www.ers.usda.gov/data-products/wheat-data/`

van Ittersum, M. K., van Bussel, L. G. J., Wolf, J., Grassini, P., van Wart, J., Guilpart, N., ... Cassman, K. G. (2016). Can sub-Saharan Africa feed itself? *Proceedings of the National Academy of the Sciences of the United States of America*, *113*, 14964–14969. doi: 10.1073/pnas.1610359113

Vandermeer, J. (1998). Maximizing crop yield in alley crops. *Agroforestry Systems*, *40*, 199–206. doi: 10.1023/A:1006072303989

Vercruyssen, L., Tognetti, V. B., Gonzalez, N., Dingenen, J. V., Milde, L. D., Bielach, A., ... Inze, D. (2015). Growth regulating factor5 stimulates arabidopsis chloroplast division, photosynthesis, and leaf longevity. *Plant Physiol.*, *167*, 817–832. doi: 10.1104/pp.114.256180

Vico, G., & Porporato, A. (2011). From rainfed agriculture to stress-avoidance irrigation: II. Sustainability, crop yield, and profitability. *Advances in Water Resources*, *34*, 272–281. doi: 10.1016/j.advwatres.2010.11.011

Wang, Huang, J., Nie, L., Wang, F., Ling, X., Cui, K., ... Peng, S. (2017). Integrated crop management practices for maximizing grain yield of double-season rice crop. *Scientific Report*, *7*, 38982. doi: 10.1038/srep38982

Wang., L., & Shangguan, Z. (2015). Photosynthetic rates and kernel-filling processes of big-spike wheat (*Triticum aestivum* L.) during the growth period, New Zealand. *Journal of Crop and Horticultural Science*, *43*, 182–192. doi: 10.1080/01140671.2014.994644

Ward, P., Palta, J. A., & Waddell, H. A. (2011). Root and shoot growth by seedlings of annual and perennial medic, and annual and perennial wheat. *Crop and Pasture Science*, *62*, 367–373. doi: 10.1071/CP10392

Webber, H., Martre, P., Asseng, S., Kimball, B., White, J., Ottman, M., ... Ewert, F. (2017). Canopy temperature for simulation of heat stress in irrigated wheat in a semi-arid environment: A multi-model comparison. *Field Crops Research*, *202*, 21–35. doi: 10.1016/j.fcr.2015.10.009

Weiland, R., & Smith, D. (2013). Ag decision maker. extension: File c6-80. [Computer software manual].

Wiesmeier, M., Hubner, R., & Kogel-Knabner, I. (2015). Stagnating crop yields: An overlooked risk for the carbon balance of agricultural soils? *Sci Total Environ.*, *536*, 1045–1051. doi: 10.1016/j.scitotenv.2015.07.064

Woo, D. K., & Kumar, P. (2016). Mean age distribution of inorganic soil-nitrogen.

Water Resour. Res, *52*, 5516-5536. doi: 10.1002/2015WR017799

Woo, D. K., & Kumar, P. (2017). Role of micro-topographic variability on mean age of soil nitrogen in intensively managed landscape. *Water Resour. Res*, *53*, 8404-8422. doi: 10.1002/2017WR021053

Woo, D. K., & Kumar, P. (2019). Impacts of subsurface tile drainage on age–concentration dynamics of inorganic nitrogen in soil. *Water Resour. Res*. doi: 10.1029/2018WR024139

Woo, D. K., Riley, W. J., & Wu, Y. (2020). More fertilizer and impoverished roots required for improving wheat yields and profits under climate change. *Field Crops Research*, *249*, 107756. doi: 10.1016/j.fcr.2020.107756

Zabel, F., Putzenlechner, B., & Mauser, W. (2014). Global agricultural land resources – a high resolution suitability evaluation and its perspectives until 2100 under climate change conditions. *PLoS One*, *9*, e107522. doi: 10.1371/journal.pone.0107522

Zhang, H., Wang, X., You, M., & Liu, C. (1999). Water–yield relations and water-use efficiency of winter wheat in the North China Plain. *Irrigation Science*, *19*, 37–45. doi: 10.1007/s002710050069

Figure 1.

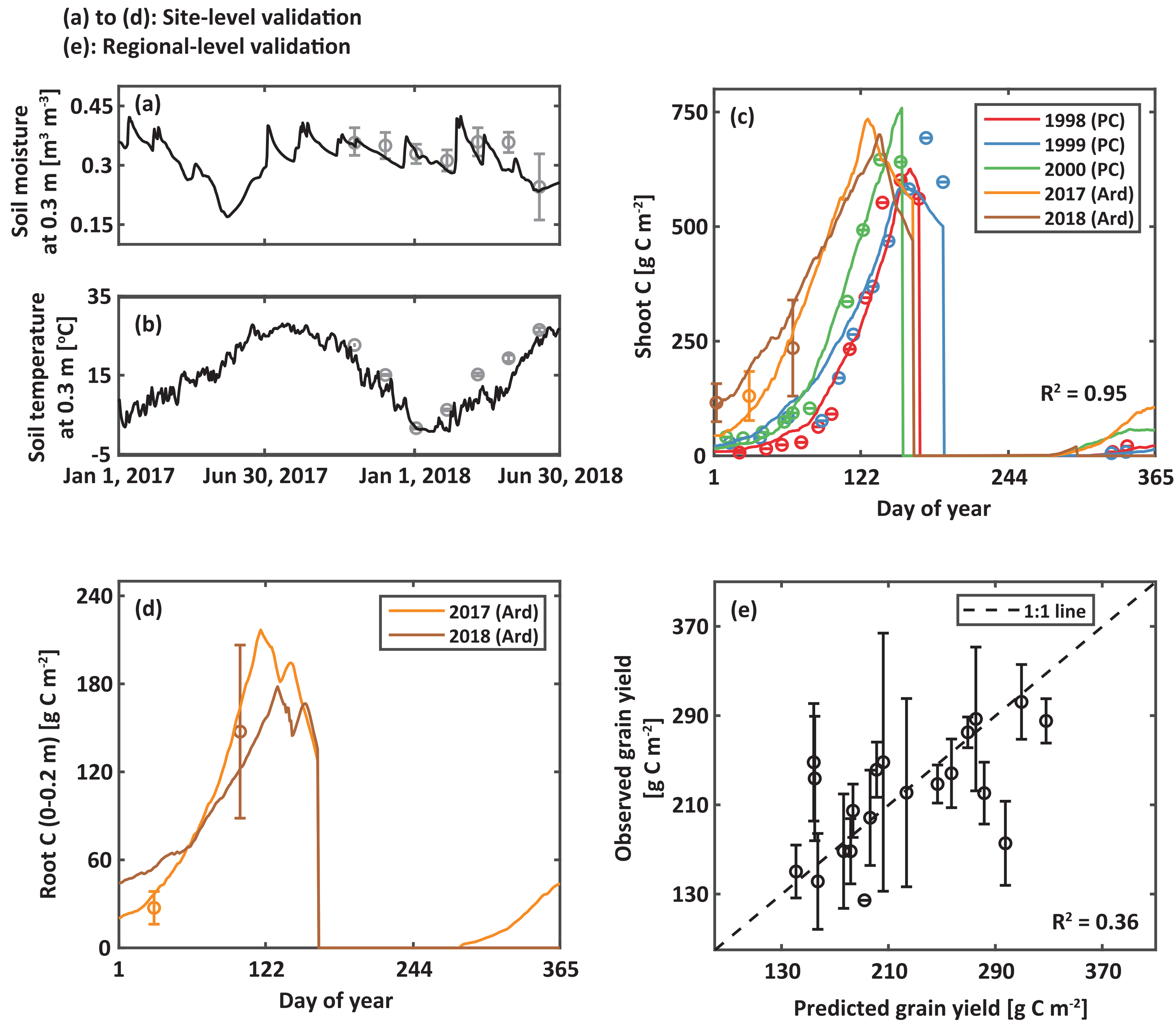
(a) to (d): Site-level validation
(e): Regional-level validation
(a)
Soil moisture at 0.3 m [m^3 m^{-3}]
0.45
0.3
0.15
(b)
Soil temperature at 0.3 m [^{o}C]
35
15
-5
Jan 1, 2017
Jun 30, 2017
Jan 1, 2018
Jun 30, 2018
(c)
Shoot C [g C m^{-2}]
750
500
250
0
1998 (PC)
1999 (PC)
2000 (PC)
2017 (Ard)
2018 (Ard)
R^2 = 0.95
1
122
244
365
Day of year
(d)
Root C (0-0.2 m) [g C m^{-2}]
240
180
120
60
0
2017 (Ard)
2018 (Ard)
1
122
244
365
Day of year
(e)
1:1 line
Observed grain yield [g C m^{-2}]
370
290
210
130
R^2 = 0.36
130
210
290
370
Predicted grain yield [g C m^{-2}]

Figure 2.

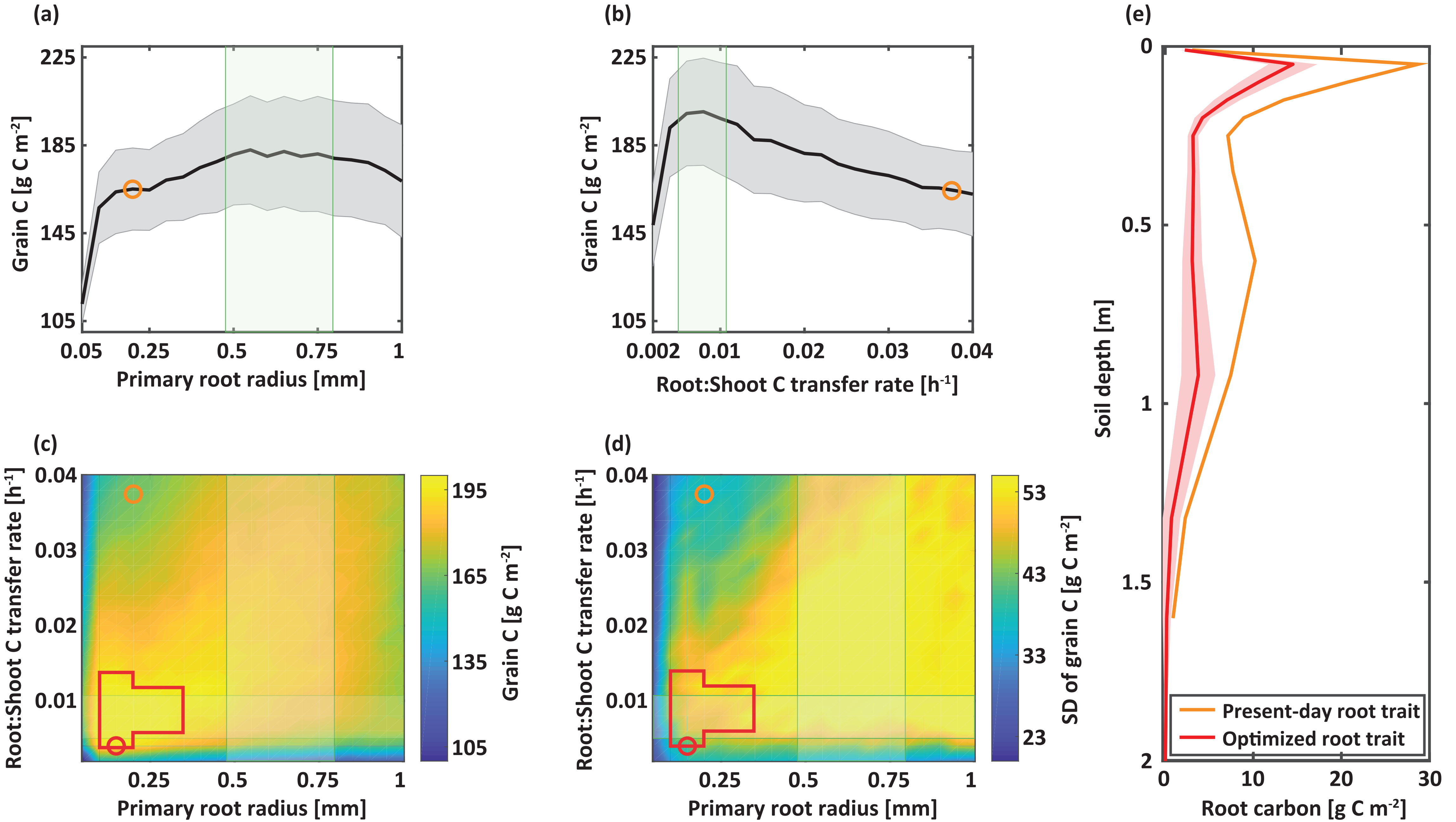
(a)
(b)
(e)
(c)
(d)
Grain C [g C m^-2]
Primary root radius [mm]
Root:Shoot C transfer rate [h^-1]
Soil depth [m]
Root carbon [g C m^-2]
SD of grain C [g C m^-2]
Present-day root trait
Optimized root trait

Figure 3.

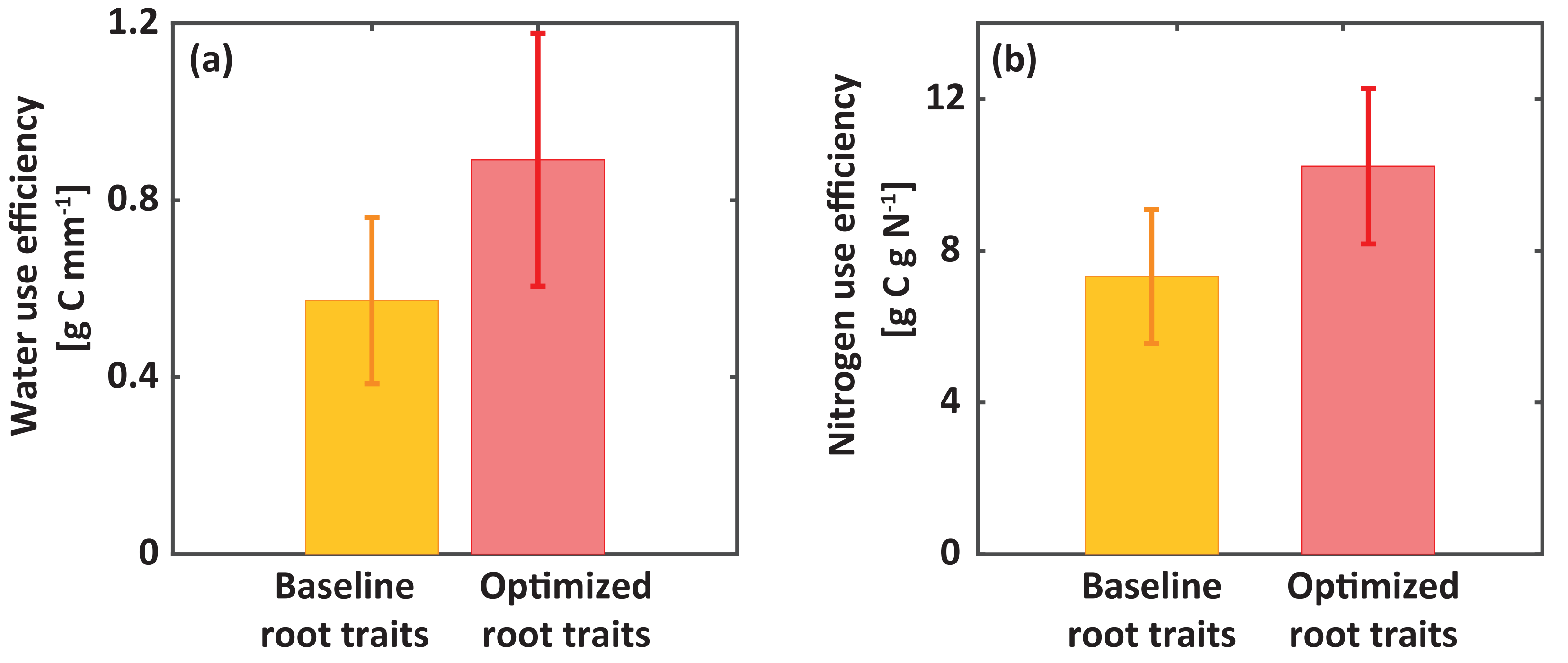

(a)
Water use efficiency [g C mm^{-1}]
1.2
0.8
0.4
0
Baseline root traits
Optimized root traits
(b)
Nitrogen use efficiency [g C g N^{-1}]
12
8
4
0
Baseline root traits
Optimized root traits

Figure 4.

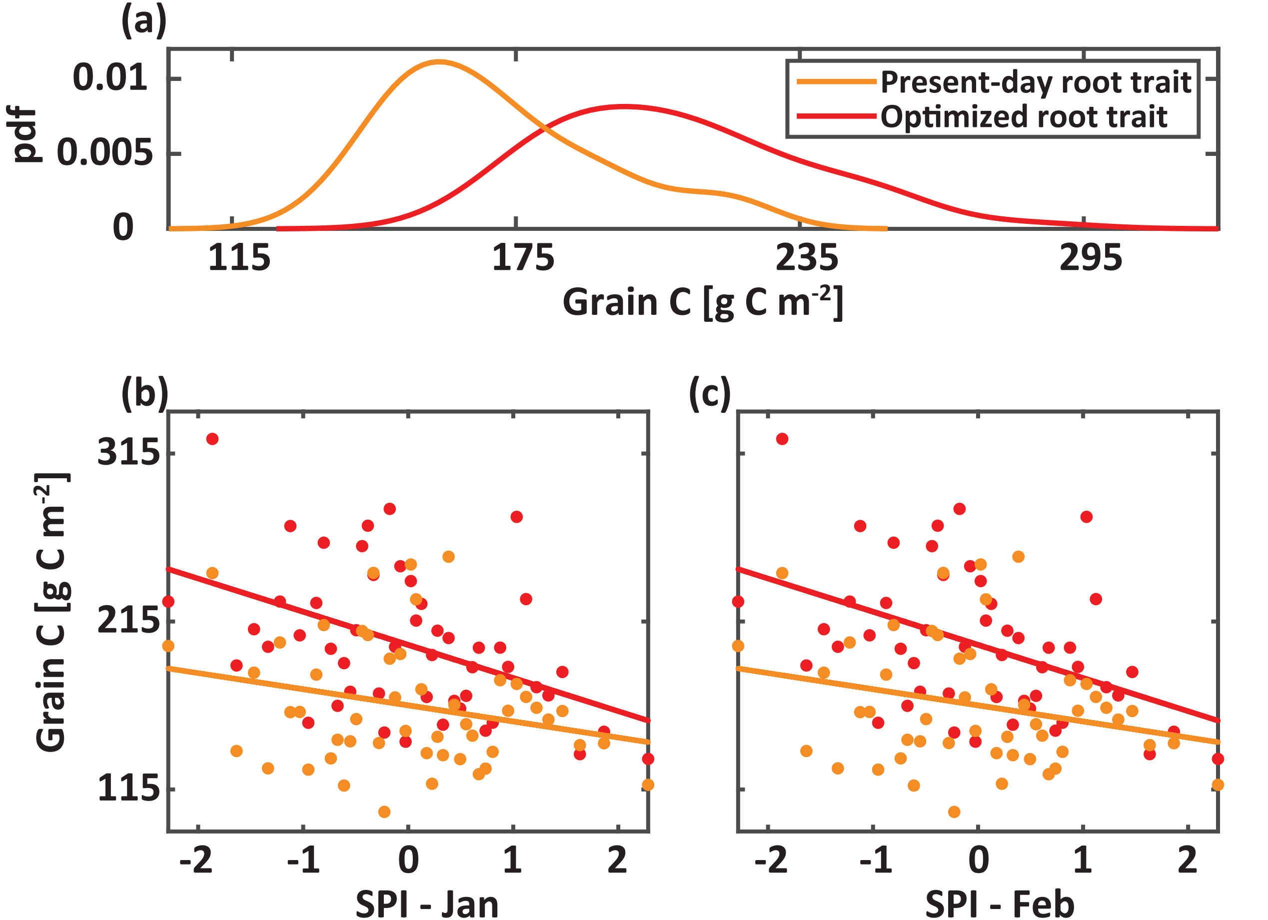

(a)
pdf
0.01
0.005
0
115
175
235
295
Grain C [g C m⁻²]
Present-day root trait
Optimized root trait
(b)
(c)
Grain C [g C m⁻²]
315
215
115
-2
-1
0
1
2
SPI - Jan
SPI - Feb

Figure 5.

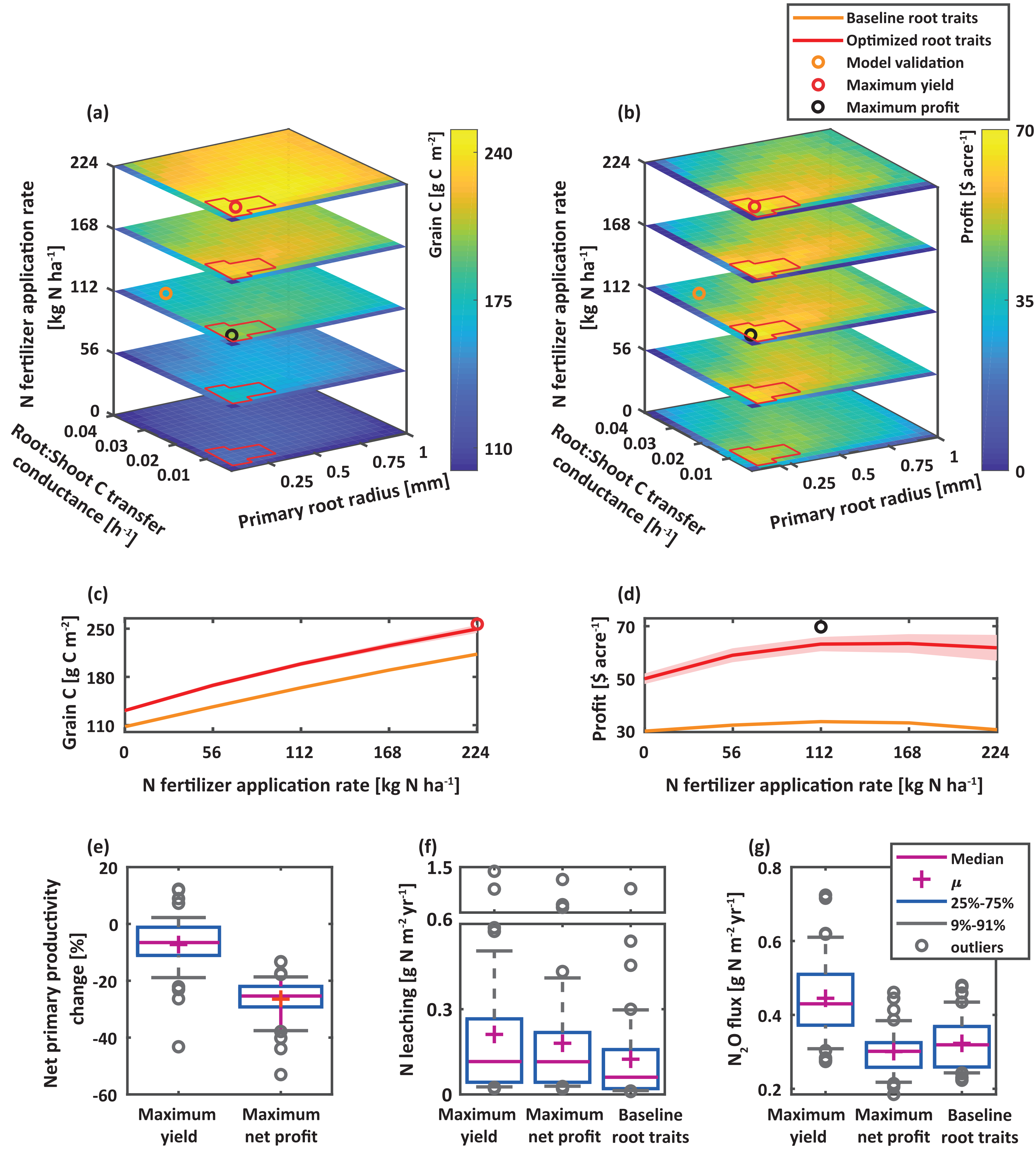

Baseline root traits
Optimized root traits
Model validation
Maximum yield
Maximum profit
(a)
(b)
N fertilizer application rate [kg N ha-1]
Grain C [g C m-2]
Profit [$ acre-1]
Root:Shoot C transfer conductance [h-1]
Primary root radius [mm]
(c)
(d)
N fertilizer application rate [kg N ha-1]
(e)
(f)
(g)
Net primary productivity change [%]
N leaching [g N m-2 yr-1]
N2O flux [g N m-2 yr-1]
Maximum yield
Maximum net profit
Baseline root traits
Median
μ
25%-75%
9%-91%
outliers

Figure 6.

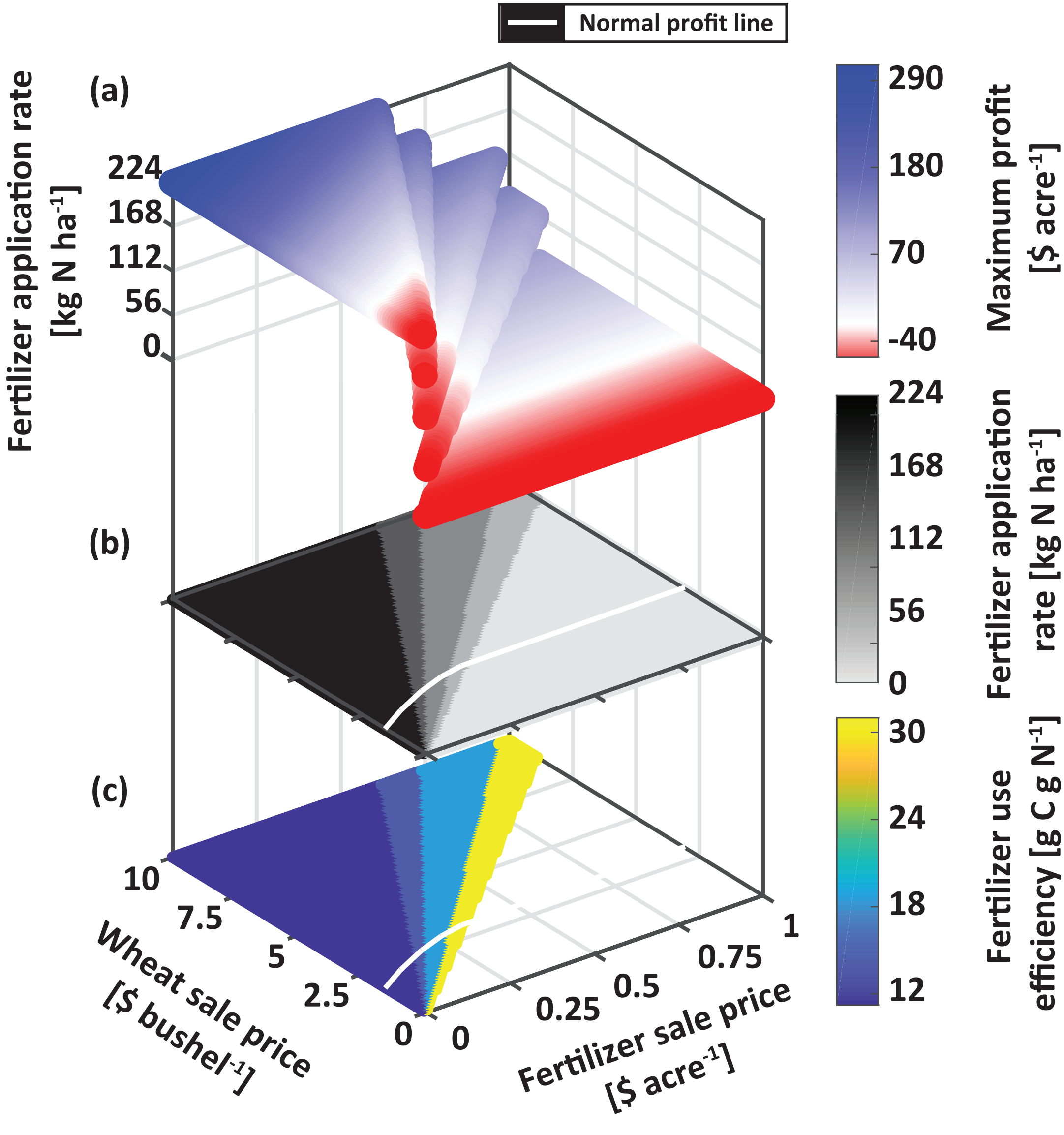
Normal profit line
(a)
(b)
(c)
Fertilizer application rate [kg N ha-1]
224
168
112
56
0
Maximum profit [$ acre-1]
290
180
70
-40
Fertilizer application rate [kg N ha-1]
224
168
112
56
0
Fertilizer use efficiency [g C g N-1]
30
24
18
12
Wheat sale price [$ bushel-1]
10
7.5
5
2.5
0
Fertilizer sale price [$ acre-1]
0
0.25
0.5
0.75
1

Figure A1.

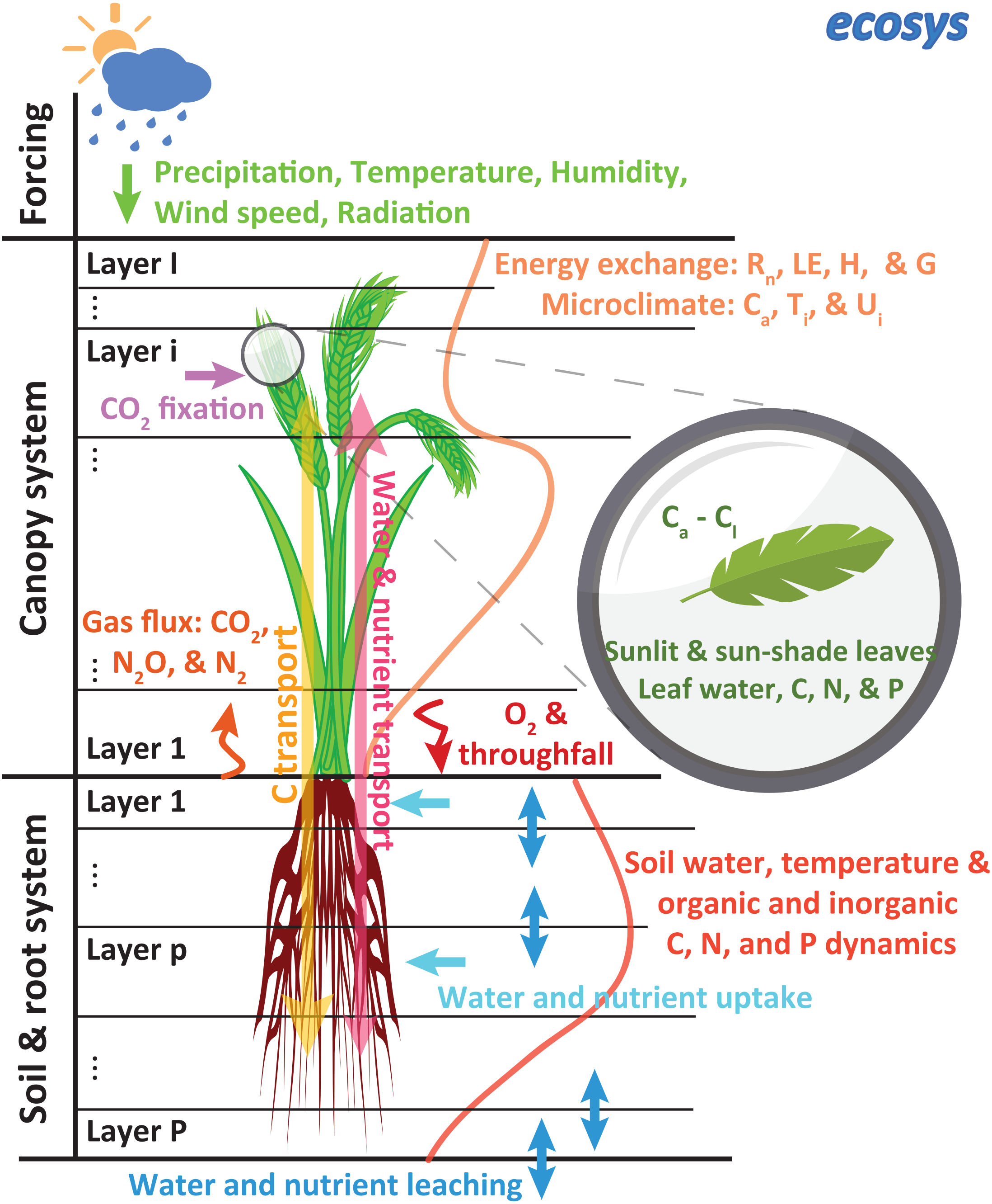

ecosys
Forcing
Precipitation, Temperature, Humidity,
Wind speed, Radiation
Canopy system
Layer l
Layer i
CO2 fixation
Energy exchange: Rn, LE, H, & G
Microclimate: Ca, Ti, & Ui
Ca - Cl
Sunlit & sun-shade leaves
Leaf water, C, N, & P
Gas flux: CO2, N2O, & N2
C transport
Water & nutrient transport
O2 & throughfall
Layer 1
Soil & root system
Layer 1
Layer p
Layer P
Soil water, temperature & organic and inorganic C, N, and P dynamics
Water and nutrient uptake
Water and nutrient leaching

Figure A2.

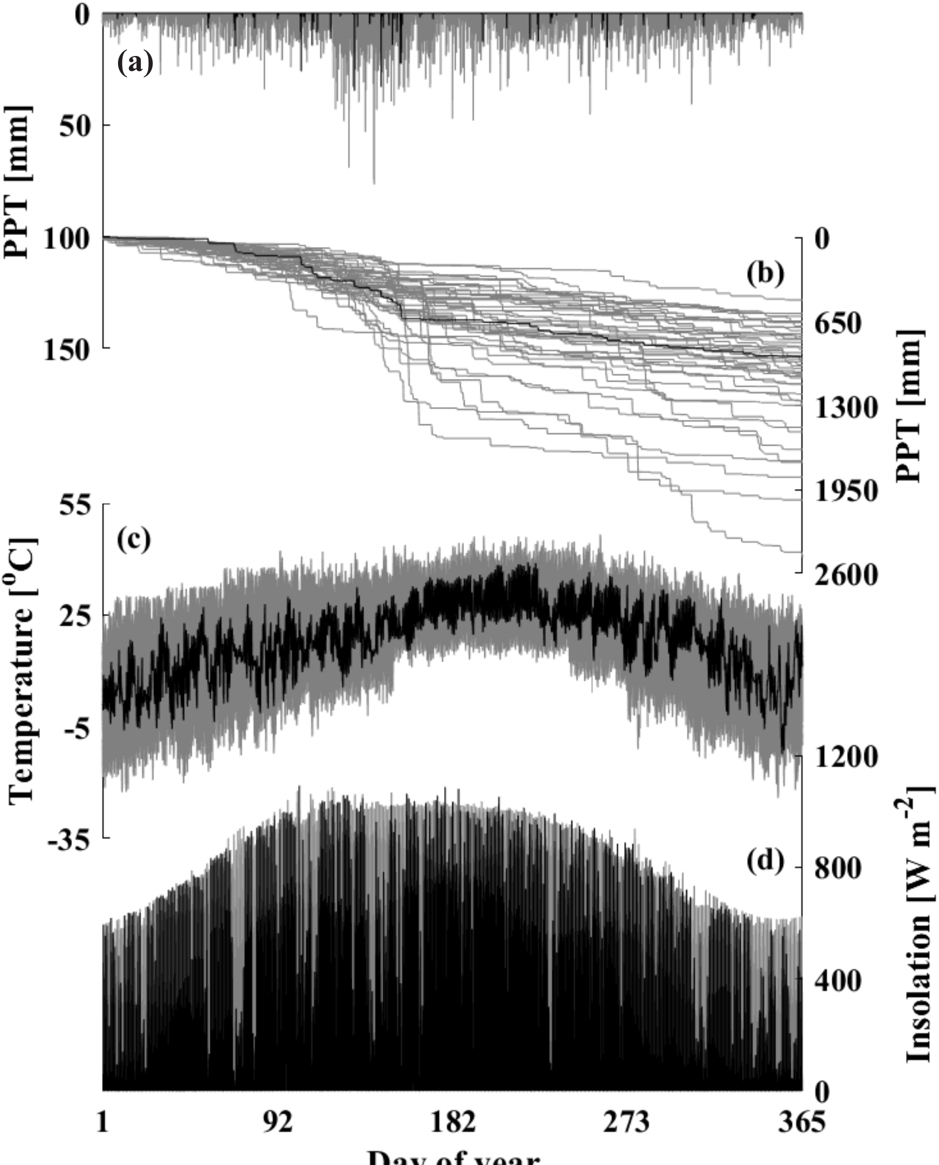

(a)
(b)
(c)
(d)
PPT [mm]
0
50
100
150
0
650
1300
1950
2600
Temperature [°C]
55
25
-5
-35
1200
800
400
0
Insolation [W m^-2]
1
92
182
273
365
Day of year

Figure A3.

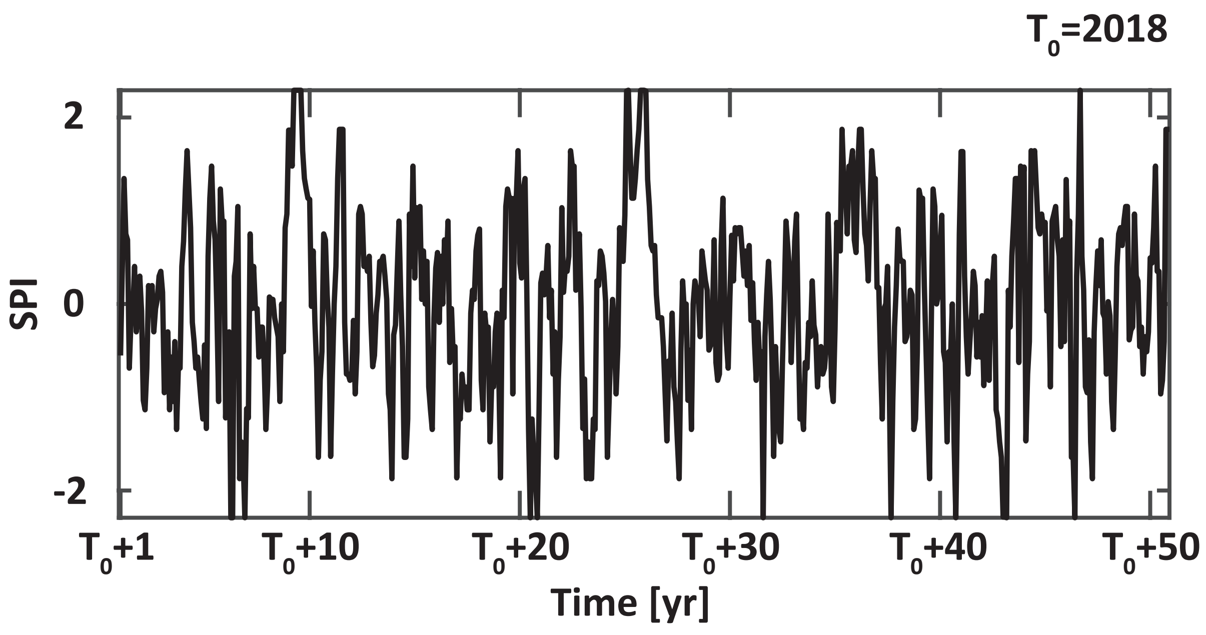

T_0=2018
SPI
2
0
-2
T_0+1
T_0+10
T_0+20
T_0+30
T_0+40
T_0+50
Time [yr]

Figure A4.

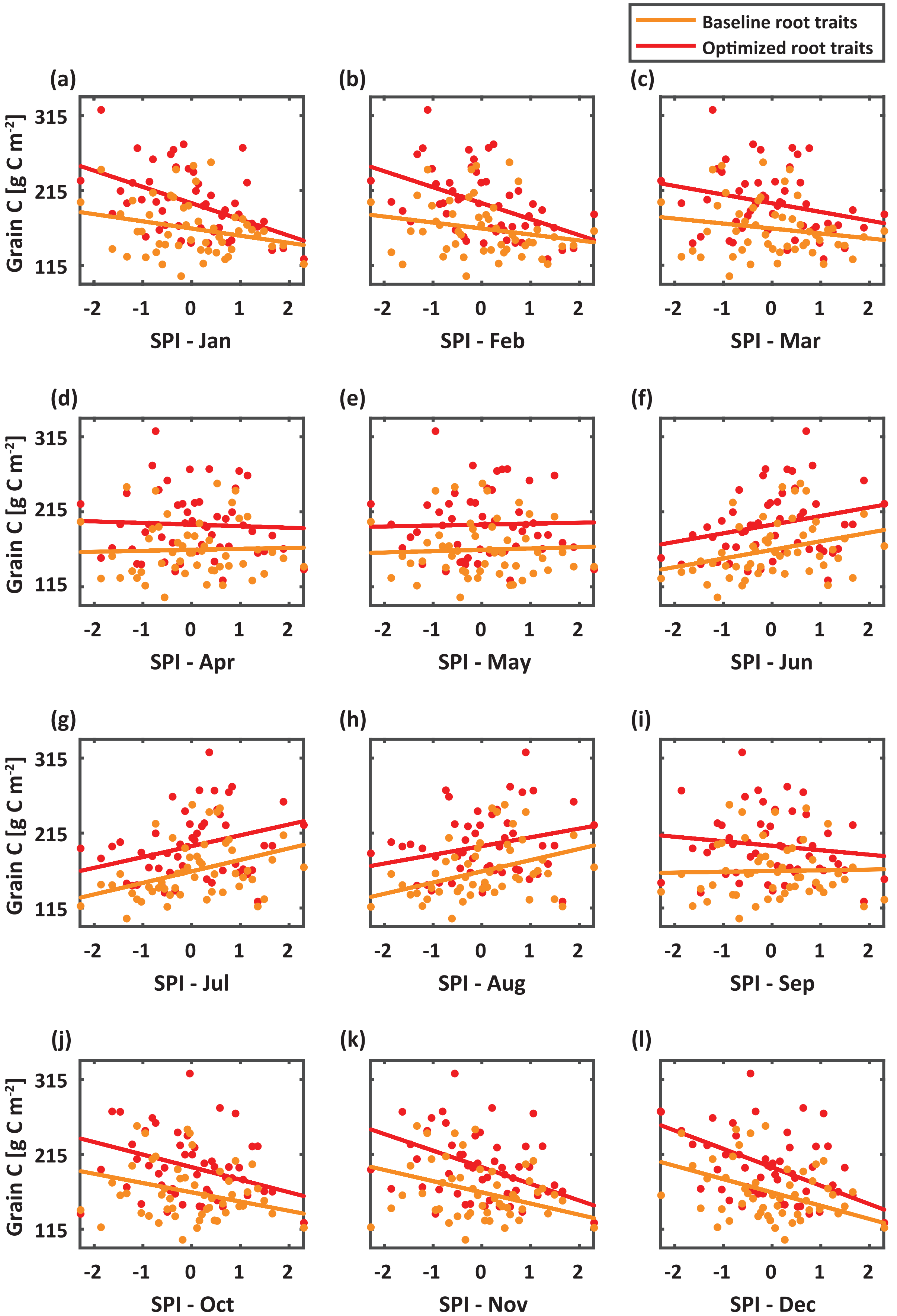

Baseline root traits
Optimized root traits
(a)
(b)
(c)
(d)
(e)
(f)
(g)
(h)
(i)
(j)
(k)
(l)
Grain C [g C m-2]
315
215
115
-2
-1
0
1
2
SPI - Jan
SPI - Feb
SPI - Mar
SPI - Apr
SPI - May
SPI - Jun
SPI - Jul
SPI - Aug
SPI - Sep
SPI - Oct
SPI - Nov
SPI - Dec

Figure A5.

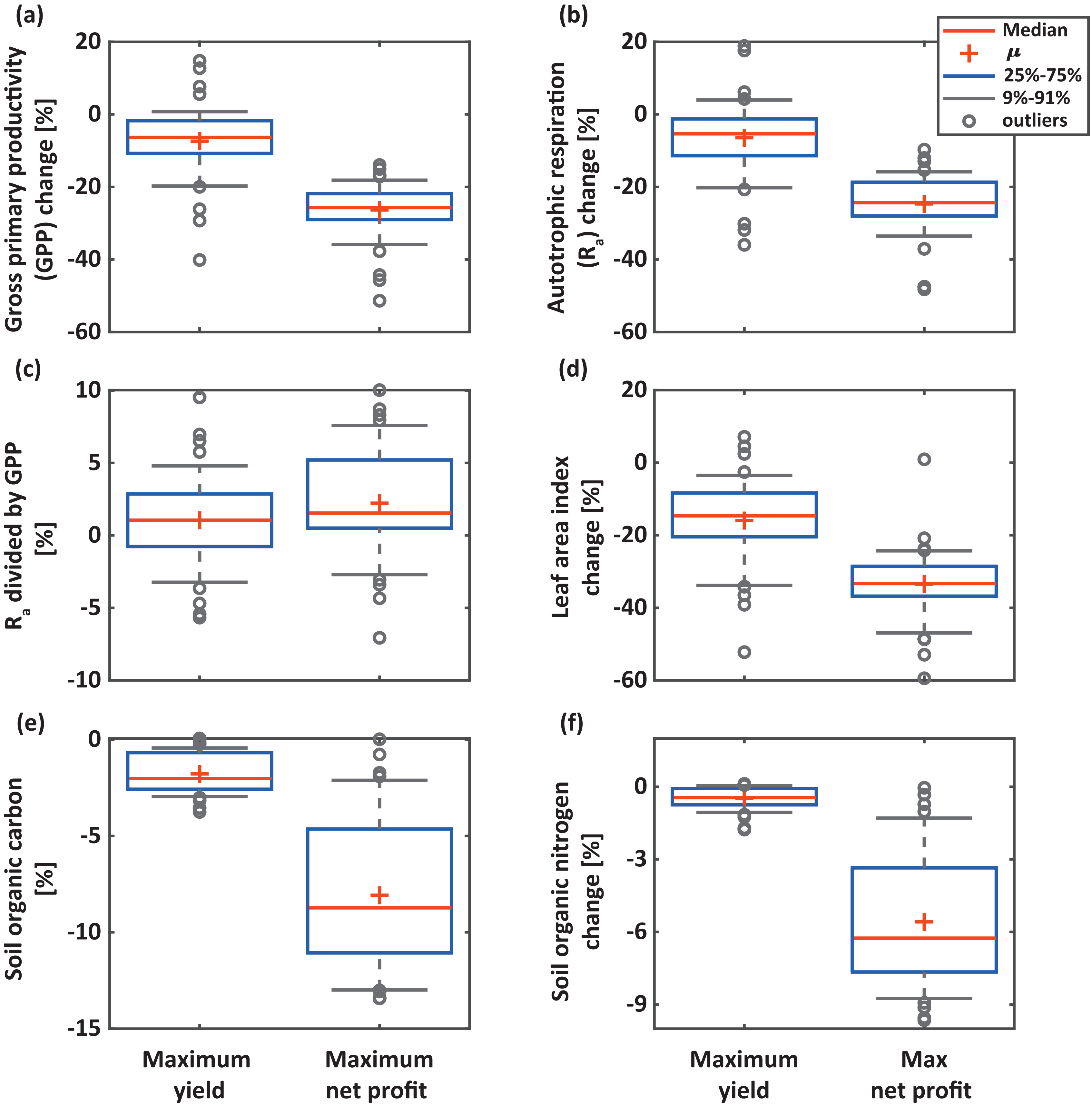
(a)
Gross primary productivity (GPP) change [%]
20
0
-20
-40
-60
(b)
Autotrophic respiration (R_a) change [%]
Median
μ
25%-75%
9%-91%
outliers
(c)
R_a divided by GPP [%]
10
5
0
-5
-10
(d)
Leaf area index change [%]
(e)
Soil organic carbon [%]
-15
(f)
Soil organic nitrogen change [%]
-3
-6
-9
Maximum yield
Maximum net profit
Max net profit